



HAL
open science

Distinct control mechanism of fine-grained sediments from Yellow River and Kyushu supply in the northern Okinawa Trough since the last glacial

Debo Zhao, Shiming Shi, Samuel Toucanne, Peter Clift, Ryuji Tada, Sidonie Révillon, Yoshimi Kubota, Xufeng Xu, Zhaojie Yu, Jie Huang, et al.

► To cite this version:

Debo Zhao, Shiming Shi, Samuel Toucanne, Peter Clift, Ryuji Tada, et al.. Distinct control mechanism of fine-grained sediments from Yellow River and Kyushu supply in the northern Okinawa Trough since the last glacial. *Geochemistry, Geophysics, Geosystems*, 2017, 18 (8), pp.2949 - 2969. 10.1002/2016GC006764 . hal-01793280

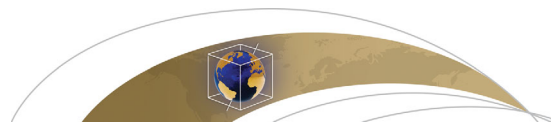
HAL Id: hal-01793280

<https://hal.science/hal-01793280>

Submitted on 12 Apr 2021

HAL is a multi-disciplinary open access archive for the deposit and dissemination of scientific research documents, whether they are published or not. The documents may come from teaching and research institutions in France or abroad, or from public or private research centers.

L'archive ouverte pluridisciplinaire **HAL**, est destinée au dépôt et à la diffusion de documents scientifiques de niveau recherche, publiés ou non, émanant des établissements d'enseignement et de recherche français ou étrangers, des laboratoires publics ou privés.



RESEARCH ARTICLE

10.1002/2016GC006764

Key Points:

- Yellow River and Kyushu Island supplied fine-grained sediments to northern Okinawa Trough since the last 34 ka
- Kuroshio Current flowed into the Okinawa Trough throughout the last 34 ka
- Sea level and Kuroshio Current system dominated the terrigenous flux from Yellow River and Kyushu Island, respectively

Supporting Information:

- Supporting Information S1
- Data Set S1

Correspondence to:

S. Wan,
wanshiming@ms.qdio.ac.cn

Citation:

Zhao, D., et al. (2017), Distinct control mechanism of fine-grained sediments from Yellow River and Kyushu supply in the northern Okinawa Trough since the last glacial, *Geochem. Geophys. Geosyst.*, 18, 2949–2969, doi:10.1002/2016GC006764.

Received 7 DEC 2016

Accepted 3 JUL 2017

Accepted article online 15 JUL 2017

Published online 9 AUG 2017

Distinct control mechanism of fine-grained sediments from Yellow River and Kyushu supply in the northern Okinawa Trough since the last glacial

Debo Zhao^{1,2} , Shiming Wan^{1,3,4} , Samuel Toucanne⁵, Peter D. Clift⁶ , Ryuji Tada⁷ , Sidonie Révillon⁸, Yoshimi Kubota⁹, Xufeng Zheng¹⁰ , Zhaojie Yu¹¹ , Jie Huang¹, Hanchao Jiang¹² , Zhaokai Xu¹ , Xuefa Shi¹³ , and Anchun Li¹

¹Key Laboratory of Marine Geology and Environment, Institute of Oceanology, Chinese Academy of Sciences, Qingdao, China, ²College of Earth Sciences, University of Chinese Academy of Sciences, Beijing, China, ³Laboratory for Marine Geology, Qingdao National Laboratory for Marine Science and Technology, Qingdao, China, ⁴Centre de Recherches Pétrographiques et Géochimiques (CRPG), CNRS-Université de Lorraine, Cedex, France, ⁵IFREMER, Unité de Recherche Géosciences Marines, Laboratoire Géophysique et Enregistrements Sédimentaires, Plouzané, France, ⁶Department of Geology and Geophysics, Louisiana State University, Baton Rouge, Louisiana, USA, ⁷Department of Earth and Planetary Science, University of Tokyo, Tokyo, Japan, ⁸SEDISOR/UMR 6538 “Domaines Oceaniques”, IUEM, Place Nicolas Copernic, Plouzané, France, ⁹Department of Geology, National Museum of Nature and Science, Ibaraki, Japan, ¹⁰Key Laboratory of Marginal Sea Geology, South China Sea Institute of Oceanology, Chinese Academy of Sciences, Guangzhou, China, ¹¹Laboratoire GEOsciences Paris-Sud (GEOPS), UMR8148, CNRS-Université de Paris-Sud, Université Paris-Saclay, Orsay Cedex, France, ¹²State Key Laboratory of Earthquake Dynamics, Institute of Geology, China Earthquake Administration, Beijing, China, ¹³Key Laboratory of Marine Sedimentology and Environmental Geology, First Institute of Oceanography, SOA, Qingdao, China

Abstract High-resolution multiproxy records, including clay minerals and Sr-Nd-Pb isotopes of the clay-sized silicate fraction of sediments from IODP Site U1429 in the northern Okinawa Trough, provide reliable evidence for distinct control mechanism on fine-grained sediments input from the Yellow River and the southern Japanese Islands to the northern Okinawa Trough since 34 ka BP. Provenance analysis indicates that the sediments were mainly derived from the Yellow River and the island of Kyushu. Since the last glacial, clay-sized sediments transported from the Yellow River to the study site were strongly influenced by sea-level fluctuation. During low sea-level stage (~34–14 ka BP), the paleo-Yellow River mouth was positioned closer to the northern Okinawa Trough, favoring large fluvial discharge or even direct input of detrital sediments, which resulted about four times more flux of clay-sized sediments supply to the study area as during the relatively high sea-level stage (~14–0 ka BP). The input of Kyushu-derived clay-sized sediments to the study site was mainly controlled by the Kuroshio Current and Tsushima Warm Current intensity, with increased input in phase with weakened Kuroshio Current/Tsushima Warm Current. Our study suggests that the Kuroshio Current was very likely flowed into the Okinawa Trough and thus influenced the fine-grained sediment transport in the area throughout the last glacial and deglacial. During ~34–11 ka BP, the Kyushu clay-sized sediment input was mainly controlled by the Kuroshio Current. Since ~11 ka BP, the occurrence of Tsushima Warm Current became important in influencing the Kyushu fine-grained sediment input to the northern Okinawa Trough.

1. Introduction

Sedimentation of suspended material transported from rivers to marginal seas can be affected by sediment supply, geomorphology, and prevailing oceanic processes (waves, tides, and currents) [Flemming, 1981; Walsh and Nittrouer, 2009]. For marginal seas characterized by wide shelves, rapid sea-level change, and ocean current evolution on geological time-scales also strongly regulates the pattern of sediments dispersal [Milliman et al., 1975; Saito et al., 1998; Shi et al., 2016; Wang, 1999]. Thus the sediments may preserve key information concerning environmental conditions, which allows us to reconstruct oceanographic evolution. Here we present a case study from the East China Sea, where the input of terrigenous sediments to the northern Okinawa Trough since the last glacial may have been significantly influenced by sea-level change, as well as the intensity of the Kuroshio Current which flows northward along the East China Sea continental

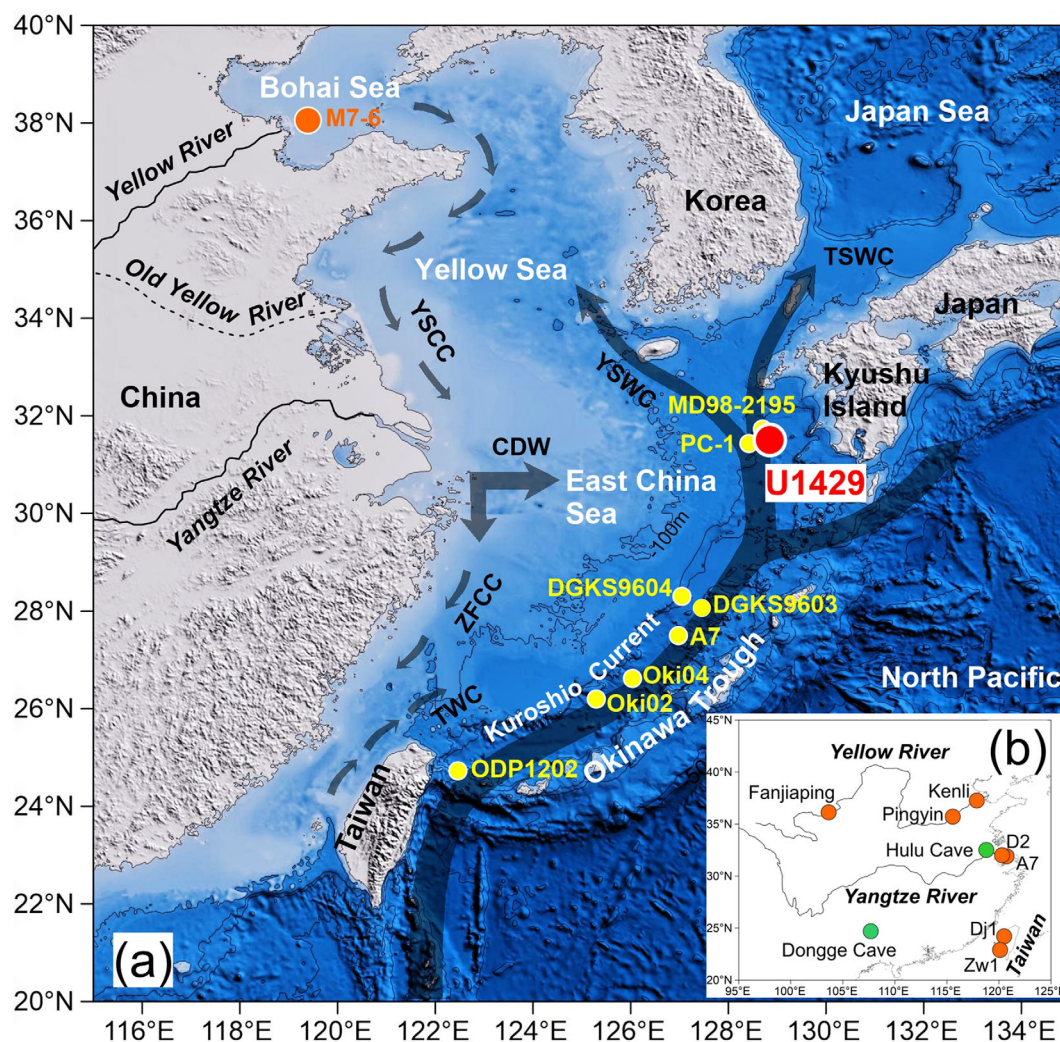


Figure 1. (a) Locations of IODP Site U1429, M7-6, and other cores referred in this study. Old Yellow River is shown from Liu *et al.* [2001]. The regional circulation pattern (translucent black arrows) in the East China Sea and adjacent areas are from Yuan *et al.* [2008]. The -100 m isobath is shown by gray line. YSCC, Yellow Sea Coastal Current; YSWC, Yellow Sea Warm Current; TSWC, Tsushima Warm Current; ECSCC, East China Sea Coastal Current; KC, Kuroshio Current; TWC, Taiwan Warm Current. (b) Sample sites locations from potential provenances in this study. Hulu and Dongge cave are from Wang *et al.* [2001] and Dykoski *et al.* [2005], respectively.

shelf break [Diekmann *et al.*, 2008; Dou *et al.*, 2010b; Lie and Cho., 2002; Xu *et al.*, 2014; Zheng *et al.*, 2014] (Figure 1a).

In order to interpret the paleoenvironmental evolution using mineralogical and detrital geochemical records, the sediment source must be well constrained. Multiple potential sediment sources and rapid changes in sea-level and ocean current during the late Quaternary resulted in distinct sedimentary provenance in the Okinawa Trough in different places and different times. During the late last glacial low sea-level stage and Holocene high sea-level stage, sediments in the southern Okinawa Trough mainly came from Taiwan [Diekmann *et al.*, 2008]. In contrast, during the last deglacial, Yangtze River and East China Sea shelf sediments input dominated this area because of increased Yangtze River fluvial runoff and sea-level rise [Diekmann *et al.*, 2008]. In the middle Okinawa Trough during the late last glacial and deglacial low sea-level stage, Yangtze River-derived sediments dominated sedimentation via paleo-Yangtze River channels on the exposed East China Sea shelf. However, a strengthened Kuroshio Current and high sea-level resulted in sediments mainly coming from Taiwan since about 7 ka BP [Dou *et al.*, 2010a,b; 2012]. In recent years, studies of the middle Okinawa Trough suggested that sediments were also derived from the Yellow River during the low sea-level in the last deglacial [Wang *et al.*, 2015; Zheng *et al.*, 2014], and Taiwan-derived

sediments transported by the Kuroshio Current could influence the middle Okinawa Trough throughout the Last Glacial Maximum (LGM) [Zheng *et al.*, 2016]. For the northern Okinawa Trough, sediments mainly came from the Yellow River, which drained through paleo-Yellow River channels on the exposed Yellow Sea and East China Sea shelves during the late last glacial and deglacial. Taiwan sediments might have been transported to this area by the strengthened Kuroshio Current since 7.3 ka BP [Li *et al.*, 2015; Xu *et al.*, 2014]. However, Kyushu is located in southern Japan (Figure 1a) and has an annual average discharge of >1.8 million tons (Mt) of suspended sediments into the northern East China Sea [Milliman and Farnsworth, 2011]. It has not been considered as a significant sediment source to the northern Okinawa Trough by previous studies [Li *et al.*, 2015; Xu *et al.*, 2014]. In contrast to the East Asian continent, Kyushu is much closer to the northern Okinawa Trough and thus has the potential to supply significant sediments to this area.

At present day, the most striking oceanographic feature in the Okinawa Trough is the Kuroshio Current, the largest western boundary current in the North Pacific, which transports warm, highly saline waters from low to middle latitudes at relatively high speed [Hu *et al.*, 2015]. Over the past two decades, a debate has existed regarding the main past pathways of the Kuroshio Current. It has been argued that the Kuroshio Current was deflected to the east part of the Okinawa Trough during the LGM and reentered the Okinawa Trough after around 7.1 ka BP [Dou *et al.*, 2012; Jian *et al.*, 1998; Ujiie and Ujiie, 1999; Ujiie *et al.*, 2003]. However, Kao *et al.* [2006] suggested that the main axis of the Kuroshio Current still flowed into the southern Okinawa Trough, and flowed out of the Karama Gap during the LGM, based on a simulation method. Sun *et al.* [2005] proposed continued influence of salty Pacific water in the Okinawa Trough transported by the Kuroshio Current throughout the last 18 ka BP based on paleoceanographic proxies. Grain-size, mineralogical, and detrital geochemical records, suggested that the Kuroshio Current remained in the Okinawa Trough since the LGM [Zheng *et al.*, 2016]. In addition, Ijiri *et al.* [2005] and Lee *et al.* [2013] proposed that the Kuroshio Current flowed into the Okinawa Trough and could have influenced the northern Okinawa Trough throughout the LGM. Furthermore, Kawahata and Ohshima [2004] found *Phyllocladus*, a kind of pollen originating in the high land of Philippines, at core MD982195 in the northern Okinawa Trough during the LGM, and thought that the Kuroshio Current was the only medium that could bring the pollen to this region during the LGM.

Previous studies were mainly focused on sediment provenance constraints on Kuroshio Current pathways using mineralogical and detrital geochemical proxies. For example, clay minerals and geochemical indices in the middle and northern Okinawa Trough revealed an increased flux of sediments from Taiwan around 8.4 or 7.3 ka BP, suggesting the reentrance of Kuroshio Current into the Okinawa Trough [Dou *et al.*, 2010b; Li *et al.*, 2015]. However, it is notable that the low sea-level during the LGM resulted in a 43% reduction of Kuroshio Current inflow [Kao *et al.*, 2006], so that the sediment transport capability by northward current would have been strongly weakened with the increasing distance from southern to the northern Okinawa Trough. As a result, the provenance signal of Taiwan was obscure especially in sediments deposited during the LGM in the northern Okinawa Trough. A Taiwan provenance signal cannot be regarded as undisputed evidence to indicate whether the Kuroshio Current flowed in or out through the northern Okinawa Trough during the glacial period. A new perspective on Kuroshio Current evolution would significantly help in understanding the evolution of the Kuroshio Current in response to climate change from the last glacial period to the Holocene.

Here we present a comprehensive, high-resolution study of the clay minerals and Sr-Nd-Pb isotopic compositions of clay-sized silicate sediments at Integrated Ocean Drilling Program (IODP) Site U1429 from the northern Okinawa Trough since 34 ka BP. The objectives of this study were to (1) constrain the provenance of clay-sized sediments in the northern Okinawa Trough and estimate the flux from each source area; (2) understand how sea-level change and ocean current evolution since the last glacial influenced the fluvial input from East Asia and from the Japanese islands to the northern Okinawa Trough; and (3) test whether Kuroshio Current flowed into or out of the Okinawa Trough during the last glacial and deglacial.

2. Materials and Methods

2.1. Core Locations and Chronological Framework

IODP Site U1429 (31°37.04'N, 128°59.85'E) is located in the northern Okinawa Trough in water depths of 732 m (Figure 1a). Three holes were cored to a composite depth below seafloor (CCSF-D) of 200 m [Tada *et al.*, 2014]. For this study, we focused on the upper 20.99 m, which spans from the late last glacial to

Table 1. Radiocarbon Dating and Linear Sedimentation Rate of IODP Site U1429 Upper 20.99 m

Depth (m)	Species	Conventional AMS ¹⁴ C Age (yr BP)	Calendar Age (cal. yr BP)	Sedimentation Rates (cm/ka)
0.35–0.37	Planktonic foraminifer mixture	1,870 ± 30	1,370 ± 35	27.2
1.85–1.87	Planktonic foraminifer mixture	6,840 ± 30	7,329 ± 35	25.2
4.78–4.80	Planktonic foraminifer mixture	10,500 ± 30	11,597 ± 35	68.6
7.33–7.35	Planktonic foraminifer mixture	12,620 ± 40	14,065 ± 44	103.3
10.56–10.58	Planktonic foraminifer mixture	16,130 ± 50	18,923 ± 53	66.5
12.06–12.08	Planktonic foraminifer mixture	17,330 ± 60	20,369 ± 63	103.7
14.06–14.08	Planktonic foraminifer mixture	19,310 ± 70	22,721 ± 72	85.0
16.72–16.74	Planktonic foraminifer mixture	23,910 ± 90	27,638 ± 92	54.1
18.47–18.49	Planktonic foraminifer mixture	25,810 ± 110	29,433 ± 111	97.7
20.97–20.99	Planktonic foraminifer mixture	30,410 ± 180	34,038 ± 181	54.3

the Holocene. The lithology of the recovered section at IODP Site U1429 is mainly calcareous nannofossil ooze and calcareous nannofossil-rich clay, within which two tephra layers were found at 17.59–18.04 m and 2.15–3.0 m. These tephra layers correspond to the Aira-Tanzawa (A-T) and Kikai-Akahoya (K-Ah) tephras commonly found in sediment cores around Japan [Chang et al., 2015; Kubota et al., 2010; Xu et al., 2014]. In order to constrain the sediment provenance, additional samples were taken from Core M7-6 (38°24'N, 119°29'E) (Figure 1a) near the Yellow River mouth in the Bohai Sea, and from surface samples from the Yellow River lower reach (two samples), from the Yangtze River mouth (two samples), from the Zengwen and Dajia Rivers in western Taiwan (two samples), and two LGM loess samples from the Lanzhou Fanjiaping sequence [Jiang et al., 2009] on the Loess Plateau. These samples were analyzed for clay mineralogy and/or isotopes composition (Figure 1b).

The age model for IODP Site U1429 was built on the basis of ten accelerator mass spectrometry (AMS) ¹⁴C dates measured by Beta Analytic Inc. Radiocarbon dates were performed on mixed planktonic foraminifera from 10 fine-grained sediment layers (Table 1). All radiocarbon ages were calibrated using software Calib Rev 7.0.4 based on the marine calibration data set Marine13 [Reimer et al., 2013] with an adjustment for a regional ¹⁴C reservoir age ($\Delta R = 39 \pm 18$) [Yoneda et al., 2007]. Between age control points, ages were linearly interpolated assuming constant sedimentation rates. The established age model reveals that the cored sediments extend to approximately 34.04 ka BP, with an average sedimentation rate of about 68.5 cm/ka (Figure 2). The age model for Core M7-6 was established by Liu et al. [2010], who indicated that the core extends to approximately 14.7 ka BP.

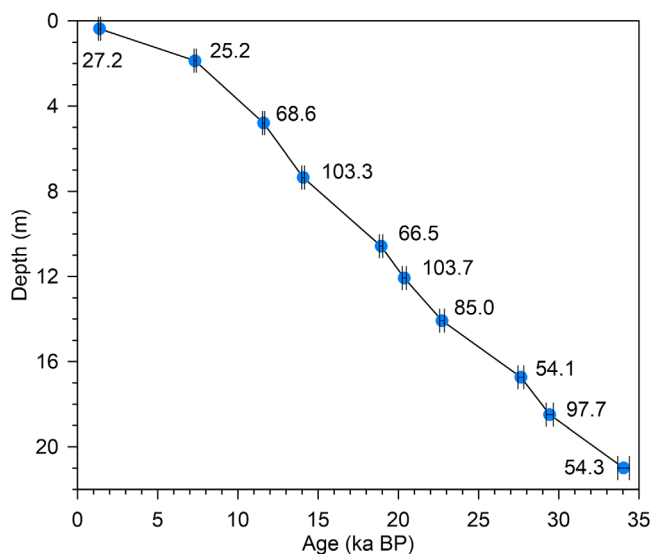


Figure 2. Calendar age and linear sediments rate of IODP Site U1429. The 10 Accelerator Mass Spectrometry (AMS) ¹⁴C dates of planktonic foraminifera samples are shown with an uncertainty of 2σ.

2.2. Analytical Methods

For clay minerals, a total of 420 samples from IODP Site U1429 were taken continuously at 5 cm intervals from the upper 20.99 m of the core. Clay mineral studies were carried out on the <2 μm fractions, which were separated based on the Stoke’s settling velocity principle and recovered by centrifuging [Dane et al., 2002; Wan et al., 2012] after removal of organic matter and carbonate by treatment with hydrogen peroxide (15%) and acetic acid (25%), respectively. The extracted clay minerals were smeared on glass slides after being fully dispersed by an ultrasonic cleaner, after which they were dried at room temperature. Clay minerals analysis was conducted by X-ray diffraction (XRD) using a D8 ADVANCE diffractometer

with CuK α (alpha) radiation (40 kV, 40 mA) in the laboratory of the Institute of Oceanology, Chinese Academy of Sciences (IOCAS). Identification of clay minerals was made according to the position of the (001) series of basal reflections on the three XRD diagrams [Moore and Reynolds, 1989]. Semiquantitative estimates of peak areas of the basal reflection for the main clay minerals groups (smectite-17 Å, illite-10 Å, and kaolinite/chlorite-7 Å) were carried out on the glycolated samples using Topas 2P software with the empirical factors of Biscaye [1965]. Replicate analysis of the same sample produced results with a relative error margin of $\pm 5\%$.

The Sr-Nd-Pb isotopic compositions of clay-sized silicate fractions were determined on 12 samples from IODP Site U1429 and 8 samples from the potential sources (Yangtze River, Yellow River, Loess Plateau, and western Taiwanese rivers) (Figure 1b). In addition, six clay-sized samples from Core M7-6 were analyzed for Sr-Nd isotopes. Clay-sized silicate fractions were extracted by the same procedure as for the clay mineral analysis. After the extraction, about 200 mg of clay-sized sample were weighted and dissolved in Savillex beakers in a mixture of ultrapure quartex HF (24 mol/L), HNO₃ (14 mol/L), and HClO₄ (12 mol/L) for 4 days at 160°C on a hot plate. After evaporation to dryness samples were dissolved in aqua regia and heated for 24 h at 130°C. Sr, Nd, and Pb fractions were chemically separated following conventional column chemistry procedures described in Révillon *et al.* [2011]. Sr and Nd isotope compositions were measured in static mode on a Thermo TRITON at the PSO (Pôle de Spectrométrie Océan) in Brest, France. All measured Sr and Nd ratios were normalized to $^{86}\text{Sr}/^{88}\text{Sr} = 0.1194$ and $^{146}\text{Nd}/^{144}\text{Nd} = 0.7219$, respectively. During the course of analysis, Sr isotope compositions of the standard solution NBS987 gave $^{87}\text{Sr}/^{86}\text{Sr} = 0.710259 \pm 7$ ($n = 9$, recommended value 0.710250); Nd standard solution La Jolla gave 0.511852 ± 2 ($n = 3$, recommended value 0.511850) and JNdi gave 0.512102 ± 6 ($n = 3$, recommended value 0.512100). Pb isotopic compositions analyses were performed at the PSO in Brest, France using a Neptune Multi-collector Inductively Coupled Plasma Mass Spectrometer (MC-ICPMS). Pb isotope ratios were corrected for instrumental mass fractionation. Machine bias was corrected by the Tl doping method of White *et al.* [2000]. Besides, SRM981 Pb standard bracketing was executed every three samples. Pb isotope reproducibility, based on 21 replicate analyses of NIST SRM981 is 0.0011 (2δ) for $^{206}\text{Pb}/^{204}\text{Pb}$ and $^{207}\text{Pb}/^{204}\text{Pb}$ and 0.0032 (2δ) for $^{208}\text{Pb}/^{204}\text{Pb}$.

Furthermore, the terrigenous materials of 95 samples were extracted by removal of the organic matters, carbonate and biogenic silica by hydrogen peroxide (15%), hydrochloric acid (0.5 mol/L), and sodium carbonate (2 mol/L), respectively [Wang *et al.*, 2015]. Dry bulk density (DBD) data were calculated based on the gamma ray attenuation bulk density and moisture content obtained onboard. The weight percent total mass accumulation rate (MAR) and terrigenous material MAR ($\text{g}/\text{cm}^2/\text{ka}$) were calculated according to the method of Rea and Janecek [1981]. Using these accumulation rates, dilution effects by other components were excluded, and furthermore, burial-related sediment compaction was corrected for Rea and Janecek [1981].

3. Results

3.1. Clay Minerals

Downcore variations of clay minerals assemblages at IODP Site U1429 are shown in Figure 3. The clay minerals assemblages are dominated by illite (35–65%) and smectite (16–51%), while chlorite (6–18%) and kaolinite (1–12%) are less abundant. From ~ 34 to 19 ka BP, the illite and chlorite contents increased slightly on a long-term trend, except for an abrupt change for the chlorite around 29 (A-T tephra layer). Besides, the illite content suggests an obvious fluctuation from ~ 22 to 19 ka BP. The smectite and kaolinite display opposite trends from ~ 34 to 19 ka BP. Two fluctuations around 29 (A-T tephra layer) and 23 ka BP have been found for smectite and kaolinite. From ~ 19 to 13 ka BP, the smectite and chlorite contents show an increasing pattern generally, whereas illite and kaolinite contents decreased gradually during this period. The chlorite content decreased from ~ 13 to 9 ka BP, and then showed an increasing trend since 9 ka BP. The illite content presents an increasing pattern since 13 ka BP. In contrast, smectite shows an overall decreasing trend over the last 13 ka BP. The kaolinite content increased significantly from ~ 13 to 9 ka BP, and then displayed a decreasing trend since 9 ka BP. All the clay minerals display significant fluctuations around ~ 9 to 8 ka BP, which corresponds to the K-Ah tephra layer (Figure 3).

The illite chemical index varies between 0.18 and 0.59, with an average value of 0.39 (Figure 3), indicating that illite was formed in an environment dominated by strong physical erosion [Esquevin, 1969; Wan

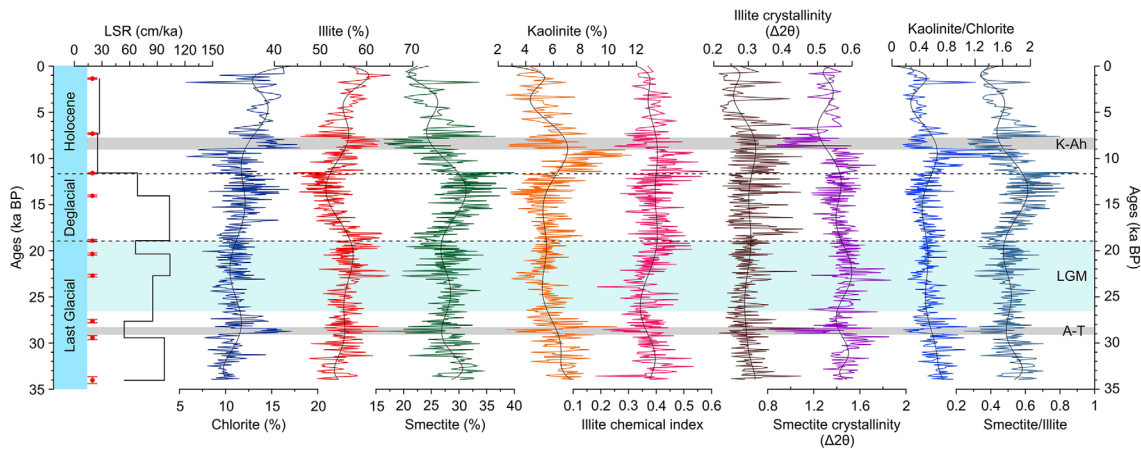


Figure 3. Variations of clay mineral parameters and liner sedimentation rate (LSR) in the terrigenous sediments from IODP Site U1429 during the last 34 ka BP are shown. Black lines are polynomial fits (degree: 10) shown to highlight general long-term trends from the original data sets. The gray bars show two tephra layers, i.e., Kikai-Akahoya (K-Ah) and Aira-Tanzawa (AT) [Arakawa *et al.*, 1998; Kitagawa *et al.*, 1995]. The dash lines show the boundaries of last glacial, deglacial, and Holocene. Blue bar shows the LGM. Red dots show 10 Accelerator Mass Spectrometry (AMS) ¹⁴C dates with an uncertainty of 2σ.

et al., 2012]. The crystallinities of illite and smectite vary between 0.21–0.60° Δ2θ and 0.81–1.87° Δ2θ, with average values of 0.30° and 1.42° Δ2θ, respectively. According to the crystallinity categories of Ehrmann [1998], such illite has very good crystallinity, and smectite has good crystallinity. Illite chemical index shows similar variations with kaolinite content. Smectite crystallinity shows fluctuations around 29 ka BP (A-T tephra layer) and ~9–8 ka BP (K-Ah tephra layer), whereas crystallinity of illite shows no obvious downcore variation (Figure 3).

3.2. Sr-Nd-Pb Isotopes

The Sr-Nd-Pb isotopic compositions measured on the clay-sized fractions of terrigenous sediments from IODP Site U1429 are shown in Figure 4 and Table 2. ε_{Nd(0)} gradually decreased from ~34 to 19 ka BP and again ~11 to 0 ka BP, but increased between ~19 and 11 ka BP. The ⁸⁷Sr/⁸⁶Sr values varied synchronously

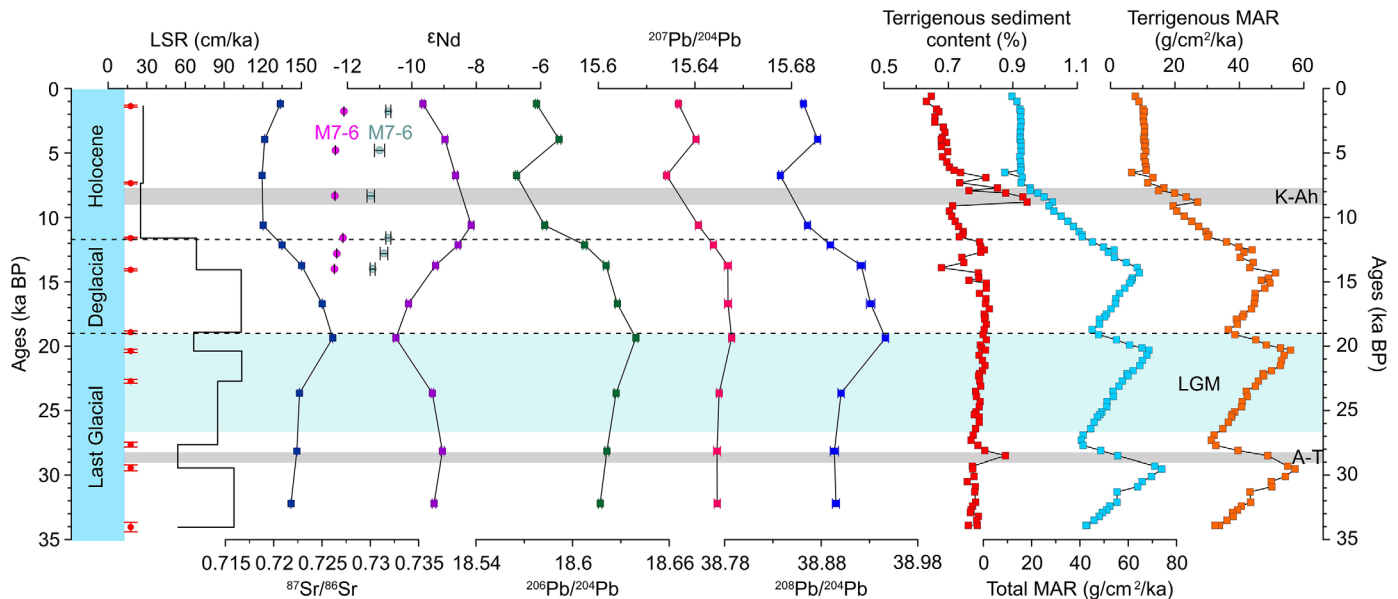


Figure 4. Variations of clay-sized particles ε_{Nd(0)}, ⁸⁶Sr/⁸⁷Sr, and Pb isotopic compositions, liner sedimentation rate (LSR), terrigenous sediments content, total MAR, and terrigenous MAR in the terrigenous sediments from IODP Site U1429 during the last 34 ka BP. Clay-sized particles ε_{Nd(0)}, ⁸⁶Sr/⁸⁷Sr isotopic compositions from Core M7-6 since 14.7 ka BP are also shown. All the isotopic results error bars are dotted with multiplier 3. The gray bars show two tephra layers, i.e., Kikai-Akahoya (K-Ah) and Aira-Tanzawa (AT). The dash lines show the boundaries of last glacial, deglacial and Holocene. Blue bar shows the LGM. Red dots show 10 Accelerator Mass Spectrometry (AMS) ¹⁴C dates with an uncertainty of 2σ.

Table 2. Clay-Sized Sediments Sr-Nd-Pb Isotopic Data of IODP Site U1429, Core M7-6 and Potential Source Areas

Samples Sites	Depth (m)	Age (ka BP)	$^{87}\text{Sr}/^{86}\text{Sr}$ ($\pm 2\sigma \times 10^{-6}$)	$^{143}\text{Nd}/^{144}\text{Nd}$ ($\pm 2\sigma \times 10^{-6}$)	$\epsilon_{\text{Nd}(0)}^a$ ($\pm 2\sigma$)	$^{206}\text{Pb}/^{204}\text{Pb}$ ($\pm 2\sigma \times 10^{-3}$)	$^{207}\text{Pb}/^{204}\text{Pb}$ ($\pm 2\sigma \times 10^{-3}$)	$^{208}\text{Pb}/^{204}\text{Pb}$ ($\pm 2\sigma \times 10^{-3}$)	
IODP Site U1429	0.32	1.19	0.720688 ± 2	0.512143 ± 2	-9.7 ± 0.04	18.578 ± 1	15.633 ± 1	38.862 ± 2	
	1.02	3.95	0.719070 ± 4	0.512178 ± 4	-9.0 ± 0.08	18.592 ± 1	15.640 ± 1	38.876 ± 3	
	1.72	6.73	0.718809 ± 3	0.512195 ± 3	-8.6 ± 0.06	18.565 ± 1	15.628 ± 1	38.838 ± 2	
	4.12	10.61	0.718901 ± 4	0.512220 ± 4	-8.2 ± 0.08	18.583 ± 1	15.641 ± 1	38.866 ± 3	
	5.35	12.13	0.720857 ± 3	0.512199 ± 3	-8.6 ± 0.06	18.607 ± 1	15.648 ± 1	38.889 ± 3	
	7.00	13.73	0.722894 ± 4	0.512163 ± 3	-9.3 ± 0.06	18.621 ± 2	15.654 ± 1	38.921 ± 4	
	9.10	16.70	0.725024 ± 4	0.512120 ± 3	-10.1 ± 0.06	18.628 ± 1	15.654 ± 1	38.931 ± 4	
	11.03	19.36	0.726108 ± 2	0.512100 ± 4	-10.5 ± 0.08	18.639 ± 1	15.655 ± 1	38.947 ± 3	
	14.58	23.65	0.722673 ± 3	0.512158 ± 2	-9.4 ± 0.04	18.627 ± 1	15.650 ± 1	38.901 ± 3	
	17.24	28.15	0.722400 ± 3	0.512174 ± 3	-9.1 ± 0.06	18.621 ± 1	15.649 ± 1	38.894 ± 4	
	19.99	32.20	0.721792 ± 3	0.512161 ± 3	-9.3 ± 0.06	18.617 ± 1	15.649 ± 1	38.895 ± 4	
	Tephra layer	2.47	~8	0.712255 ± 4	0.512398 ± 3	-4.7 ± 0.06	18.512 ± 1	15.613 ± 1	38.720 ± 4
	Core M7-6	0.80	1.78	0.727273 ± 6	0.512088 ± 4	-10.7 ± 0.08	-	-	-
1.60		4.80	0.726397 ± 6	0.512074 ± 8	-11.0 ± 0.16	-	-	-	
2.20		8.32	0.726337 ± 8	0.512060 ± 6	-11.3 ± 0.12	-	-	-	
3.20		11.59	0.727171 ± 4	0.512088 ± 4	-10.7 ± 0.08	-	-	-	
3.60		12.80	0.726525 ± 8	0.512081 ± 6	-10.9 ± 0.12	-	-	-	
4.00		14.01	0.726281 ± 6	0.512063 ± 4	-11.2 ± 0.08	-	-	-	
Yangtze River D2	Surface sediment	-	0.729081 ± 3	0.512085 ± 3	-10.8 ± 0.06	18.600 ± 1	15.656 ± 1	38.838 ± 3	
Yangtze River A7	Surface sediment	-	0.732188 ± 3	0.512100 ± 3	-10.5 ± 0.06	18.683 ± 1	15.678 ± 1	38.910 ± 3	
Yellow River (Pingyin)	Surface sediment	-	0.726059 ± 4	0.512049 ± 3	-11.5 ± 0.06	18.629 ± 2	15.646 ± 2	38.855 ± 4	
Yellow River (Kenli)	Surface sediment	-	0.725603 ± 3	0.511960 ± 4	-13.2 ± 0.08	18.597 ± 1	15.641 ± 1	38.846 ± 4	
Taiwan River (Zw1)	Surface sediment	-	0.723361 ± 4	0.512029 ± 4	-11.9 ± 0.08	18.528 ± 1	15.666 ± 1	38.826 ± 3	
Taiwan River (Dj1)	Surface sediment	-	0.721102 ± 3	0.512134 ± 3	-9.8 ± 0.06	18.615 ± 1	15.685 ± 1	38.954 ± 3	
Loess (L1)	-	LGM	0.725445 ± 3	0.512042 ± 4	-11.6 ± 0.08	18.710 ± 1	15.661 ± 2	38.909 ± 5	
Loess (L2)	-	LGM	0.724374 ± 3	0.512127 ± 4	-10.0 ± 0.08	18.711 ± 1	15.662 ± 1	38.910 ± 3	

^a $\epsilon_{\text{Nd}(0)} = [(^{143}\text{Nd}/^{144}\text{Nd}_{\text{Sample}})/(^{143}\text{Nd}/^{144}\text{Nd}_{\text{CHUR}}) - 1] \times 10,000$, and $^{143}\text{Nd}/^{144}\text{Nd}_{\text{CHUR}}$ is the present-day Chondritic Uniform Reservoir (CHUR) value of 0.512638 [Jacobsen and Wasserburg, 1980]. - means data unavailable.

with the Pb isotopic compositions ($^{206}\text{Pb}/^{204}\text{Pb}$, $^{207}\text{Pb}/^{204}\text{Pb}$, and $^{208}\text{Pb}/^{204}\text{Pb}$) and gradually increased from ~34 to 19 ka BP, and decreased from ~19 to 7 ka BP. However, after ~7 ka BP, the $^{87}\text{Sr}/^{86}\text{Sr}$ ratio remained relatively stable, while Pb isotopic compositions showed a slightly positive fluctuation (Figure 4). In addition, one sample from the K-Ah tephra layer shows a more positive $\epsilon_{\text{Nd}(0)}$ and lower $^{87}\text{Sr}/^{86}\text{Sr}$, as well as lower Pb isotopic compositions ($^{206}\text{Pb}/^{204}\text{Pb}$, $^{207}\text{Pb}/^{204}\text{Pb}$, and $^{208}\text{Pb}/^{204}\text{Pb}$) (Table 2).

The $^{87}\text{Sr}/^{86}\text{Sr}$ and $\epsilon_{\text{Nd}(0)}$ values of sediment from Core M7-6 have similar fluctuation patterns with very limited variation, which increased at ~14.0–11.6 ka BP and ~8.3–1.8 ka BP, and decreased at ~11.6–8.3 ka BP (Figure 4 and Table 2).

Concerning the isotopic compositions of potential sources, the Yellow River has more negative $\epsilon_{\text{Nd}(0)}$ (average -12.4) than the Yangtze River (average -10.6), Taiwanese rivers (average -10.9) and the loess (average -10.8). The Yangtze River has the highest $^{87}\text{Sr}/^{86}\text{Sr}$, with an average value of 0.730634 compared to other potential sources, whereas Taiwanese rivers have the lowest $^{87}\text{Sr}/^{86}\text{Sr}$, with an average value of 0.722232. The Yellow River and loess have similar $^{87}\text{Sr}/^{86}\text{Sr}$ values, with averages of 0.725831 and 0.724909, respectively. For the Pb isotopes, compared with the other potential sources, the Yellow River has the lowest $^{207}\text{Pb}/^{204}\text{Pb}$ (average 15.644) and $^{208}\text{Pb}/^{204}\text{Pb}$ (average 38.850) values, and Taiwanese rivers have the lowest $^{206}\text{Pb}/^{204}\text{Pb}$ (average 18.571). In contrast, the loess has the highest $^{206}\text{Pb}/^{204}\text{Pb}$ (average 18.710) and $^{208}\text{Pb}/^{204}\text{Pb}$ (average 38.910) values (Table 2).

3.3. Terrigenous Content and MAR

The terrigenous content of IODP Site U1429 shows a stable trend from ~34 to 11 ka BP, with an average value of 79.3%. From ~11 to 0 ka BP, the terrigenous content displayed a decreasing pattern, with the average value of 67.5%. The total MAR and terrigenous MAR suggest the similar trends with the terrigenous content, and exhibit the higher MARs during the last glacial and deglacial than that in the Holocene. Temporal variations in total MAR, terrigenous content and MAR are all in phase with the linear sedimentation rate (LSR) (Figure 4).

4. Discussion

4.1. Provenance of the Clay-Sized Sediments

A prerequisite for interpretation of mineralogical and geochemical trends in marine sediments is knowledge of the potential source areas, as well as sediment transport processes [Colin *et al.*, 2006]. In previous provenance studies in the Asian marginal seas, the most common method is to assume that the modern fluvial sediments are an analogue of potential sediment sources in the geological past [Clift *et al.*, 2014; Colin *et al.*, 2006; Dou *et al.*, 2010b; Hu *et al.*, 2013; Huang *et al.*, 2011; Wan *et al.*, 2015; Yang *et al.*, 2007]. However, rivers themselves likely changed compositions in the past as their evolution was controlled by many variable processes including tectonic activity, climate change, and human disturbance [Wan *et al.*, 2015]. Therefore caution should be exercised in the use of modern river sediments as the end-member for potential provenance of offshore cores, especially when the river drainage basin (i.e., Yellow River) is known to be sensitive to environment change over the studied time scale [Hu *et al.*, 2012].

IODP Site U1429 has multiple potential sediment sources including the great rivers of East Asia (Yellow and Yangtze Rivers), as well as small mountainous rivers in nearby southern Kyushu, the Korean peninsula, and the island of Taiwan. The modern Yangtze and Yellow Rivers deliver 470 Mt and 1100 Mt of suspended sediments annually to the East Asian Marginal Seas, respectively, totally contributing about 10% of the world's annual sediment discharge [Milliman and Farnsworth, 2011]. For the Yangtze River drainage basin, although climatic factors such as temperature and monsoonal precipitation play a role, Zhang *et al.* [1990] and He *et al.* [2013] have argued that the lithologies and tectonic setting of the drainage area are the first-order controls on the isotopic composition and clay minerals assemblages of river sediments. Paleozoic carbonate rock dominates the upper reaches, while acidic-metamorphic rocks and Quaternary clastic sediments are widely distributed in the middle and lower reaches [Yang *et al.*, 2003; Zhang *et al.*, 1990]. Although the presence of different source rocks and variable chemical weathering intensity among different catchments have induced compositional variations in river sediments through the Yangtze River drainage basin, the source of sediments in the Yangtze River mouth has remained relatively stable during the Quaternary [Yang *et al.*, 2006]. In contrast, a recent study suggested that the river sediments of the Yellow River upper reach at Yinchuan-Hetao are mainly eroded from Northeast Tibet, and further these sediments are transported to the western Mu Us desert and Loess Plateau by the East Asian winter monsoon winds [Nie *et al.*, 2015]. The loess deposits, widely distributed in the upper and middle reaches of the Yellow River, occupy about half of the whole Yellow River drainage [Ren and Shi, 1986]. In addition, East Asian monsoon variability was suggested to strongly influence the mixing proportions of sediments from the different tributaries on glacial-interglacial timescales [Hu *et al.*, 2012]. As a result, the modern Yellow River probably cannot be used as a reliable analogue to constrain the sources of sediments deposited in the geological past.

The small mountainous rivers in Kyushu, the Korean peninsula, and even Taiwan are other potential sources to the Okinawa Trough. Given the high relief, steep gradients, frequent tectonic activity, heavy rainfall, and typhoons, Taiwanese rivers collectively discharge more than 300 Mt of sediments annually to the surrounding ocean [Milliman and Farnsworth, 2011]. Provenance studies indicate that Taiwan-derived sediments have been transported to the northern Okinawa Trough by the Kuroshio Current since 7.3 ka BP [Li *et al.*, 2015; Xu *et al.*, 2014]. Kyushu delivers 1.8 Mt/yr of suspended sediments via the Chikugo River to the northern East China Sea [Milliman and Farnsworth, 2011]. Plentiful rainfall on Kyushu facilitates quick transport of weathered materials to the northern Okinawa Trough [Sidle and Masahiro, 2004]. In addition, rivers in the southern Korean Peninsula including the Yeongsan, Seumjin, and Nakdong, deliver 0.7 Mt, 2 Mt, and 8.2 Mt of suspended materials annually to the Yellow Sea, respectively [Milliman and Farnsworth, 2011]. Therefore, Korean sediments also have the potential to influence the northern Okinawa Trough.

Although, previous studies suggested that eolian particles from central Asia play an important role in detrital fluxes to the pelagic Pacific Ocean [Nakai *et al.*, 1993], fluvial derived detritus overwhelms the wind-borne materials supply in the East Asian marginal seas [Dou *et al.*, 2012; Li *et al.*, 2015; Stuet *et al.*, 2002; Wan *et al.*, 2007]. As a result, the influence of eolian particles on sediment composition can be neglected.

Clay minerals have been widely used as proxies for discriminating clay-sized sediments provenance in East China Sea in recent years [Dou *et al.*, 2010a; Xu *et al.*, 2014; Yang *et al.*, 2003], despite the fact that this proxy can be sensitive to climate or anthropogenic influences [Clift, 2016]. Previous studies have documented that Yellow River has higher content of smectite than the Yangtze River [Jian Liu *et al.*, 2010; Wan *et al.*, 2007;

Table 3. Clay Mineral Contents of IODP Site U1429 and Potential Source Areas

Samples		Smectite (%)	Kaolinite (%)	Illite (%)	Chlorite (%)	References
IODP Site U1429	Holocene	26	6	55	12	This study
	Deglacial	30	6	53	12	This study
	Last glacial	28	6	56	11	This study
Yangtze River	Surface sediment	5	9	69	16	Wan et al. [2007]
	Surface sediment	6	16	66	12	Yang et al. [2003]
Yellow River	Surface sediment	12	10	62	16	Yang et al. [2003]
	Surface sediment	13	8	67	12	Ren and Shi [1986]
Old Yellow River	Surface sediment	21	8	64	8	Qin and Li [1983]
	Loess	LGM	10	6	72	13
Taiwan rivers	LGM	8	7	73	12	This study
	Surface sediment	0	1	75	24	Li et al. [2012]
East Taiwan shelf	Surface sediment	0	2	76	22	Wan et al. [2012]
	Surface sediment	6	5	62	27	Chen [1973]
East China Sea shelf	Surface sediment	6	9	65	20	Xu et al. [2009]
	Surface sediment	8.1	7.5	60.5	23.9	Chen [1973]
Ariake Bay	~2.5–0m	61	9	21	10	Ohtsubo et al. [1995]
Yeongsan River	Surface sediment	0.1	19.2	63.9	16.8	Kim [1979]
Nakdong River	Surface sediment	0.1	22.5	58.6	18.8	Park and Khim [1990]

Yang et al., 2003]. Sediments from Taiwan are enriched in illite and chlorite, with the absence of smectite and kaolinite [Wan et al., 2010]. Korean rivers also contain a small amount of smectite [Kim, 1979; Park and Khim, 1990]. In contrast, Kyushu river sediments contain abundant smectite (~61%) on account of the widely distributed active volcanoes around the Japanese islands [Ohtsubo et al., 1995] (Table 3).

In order to constrain the provenance of clay minerals sampled from IODP Site U1429, we applied a ternary diagram of (illite + chlorite)-kaolinite-smectite (Figure 5). The clay minerals assemblages of the core are compared with the reference data from potential sources including Yangtze River, Yellow River, East China Sea shelf, Taiwan, Ariake Bay in southern Kyushu, and Korean rivers. Almost all the samples of the study site plotted as a group and are subparallel to the illite + chlorite-smectite line. This trend can be interpreted as a mixture of multiple sediment sources from the Yangtze, Yellow and Taiwanese rivers and/or loess (high illite/chlorite end-member) and Kyushu (high smectite end-member). Note that the high content of smectite at the study site is difficult to reconcile without a contribution from a smectite-rich end-member (i.e., Kyushu). Kyushu is characterized by widespread Quaternary pyroclastic rocks and lavas overlying Tertiary formations [Okada et al., 2000]. Under warm (mean annual temperature 18.6°C) and humid (mean annual precipitation 2265 mm) conditions on Kyushu (data from Japan Meteorological Agency), rapid chemical weathering of volcanic rocks can produce a high abundance of smectite [Bluth and Kump, 1994; Dessert et al., 2001] and indeed the rivers of Kyushu contain abundant smectite (~61%) [Chamley, 1989; Ohtsubo et al., 1995]. Here we exclude the alteration of submarine tephra as a significant source of smectite because such volcanic materials are not strongly eroded and weathered, as it the case with subaerial sources [Aumento et al., 1976] and the tephra and surrounding layers (K-Ah and A-T) in the core are not characterized by elevated smectite contents (Figure 3). In any case, sediments from Korean rivers probably have a minor contribution, as some samples of the study site deviate to kaolinite-rich end-member.

In comparison with clay minerals, naturally occurring radiogenic isotopes, e.g., ⁸⁷Sr/⁸⁶Sr, ¹⁴³Nd/¹⁴⁴Nd, and ^{206, 207, 208}Pb/²⁰⁴Pb, are more robust indicators of sedimentary provenance because they mainly depend on lithology and rock ages [Biscaye et al., 1997]. Previous studies have demonstrated that Nd isotopes in sediments are not significantly influenced by erosion and transport compared to the original bedrock values. In

Table 4. Radiogenic Sr, Nd, and Pb Isotope Composition (Bulk Samples) and Average Concentrations (ppm) in the Potential End-Members^a

Potential Sediment Provenance	Sr (ppm)	⁸⁷ Sr/ ⁸⁶ Sr	Nd (ppm)	ε _{Nd(0)}	Pb (ppm)	²⁰⁶ Pb/ ²⁰⁴ Pb	²⁰⁷ Pb/ ²⁰⁴ Pb	²⁰⁸ Pb/ ²⁰⁴ Pb
Yellow River ^{b,c,d}	231.6	0.717019	28.5	-12.4	30.4			
Yangtze River ^{b,d,e}	80.0	0.723723	35.1	-11.7	41.6			
Taiwan rivers ^{d,f}	50.0	0.712219	30.0	-9.6	20.0			
Loess ^{g,h}	142.7	0.719958	21.4	-11.4	9.2			
Volcanic rocks ⁱ	461.0	0.704307	19.6	1.8	7.2	18.284	15.569	38.422

^aData sources: ^bMeng et al. [2008]; ^cHu et al. [2012]; ^dBentahila et al. [2008]; ^eYang et al. [2007]; ^fLin et al. [1995]; ^gYokoo et al. [2004]; ^hSun and Zhu [2010]; ⁱHosono et al. [2003].

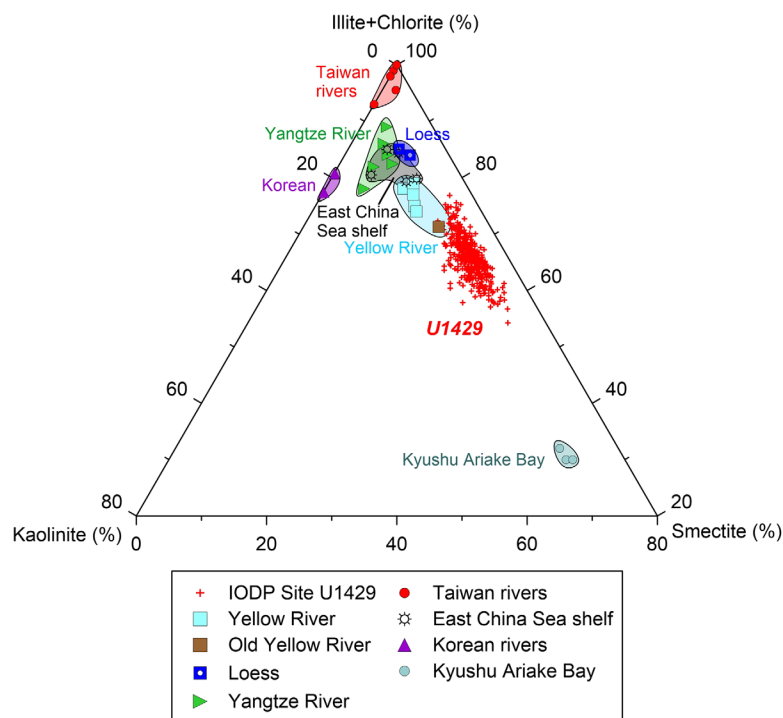


Figure 5. Provenance analysis of IODP Site U1429 sediments using a ternary diagram of (illite + chlorite)-kaolinite-smectite. Potential sources including modern Yangtze River [Fan *et al.*, 2001; Ren and Shi, 1986; Xu, 1983; Yang *et al.*, 2003; Yang, 1988] and Yellow River [Fan *et al.*, 2001; Xu, 1983; Yang *et al.*, 2003; Yang, 1988], old Yellow River [Qin and Li, 1983], East China Sea shelf [Aoki and Oinuma, 1974; Chen, 1973; Li, 1990; Xu *et al.*, 2009; Zhou *et al.*, 2010], Taiwanese rivers [Li *et al.*, 2012; Wan *et al.*, 2012], Korean rivers [Kim, 1979; Park and Khim, 1990], and Kyushu Ariake Bay [Ohtsubo *et al.*, 1995].

contrast, the Pb and Sr isotopes could be fractionated among different grain-size fractions during sedimentation and are affected by chemical weathering [Colin *et al.*, 2006; Erel *et al.*, 1994]. The preferential release of Pb from apatite, zircon, sphene, and monazite enriched in the silt fraction results in more radiogenic ^{206}Pb , ^{207}Pb , $^{208}\text{Pb}/^{204}\text{Pb}$ [Erel *et al.*, 1994]. The coarse fractions are dominated by quartz and feldspar, with low $^{87}\text{Sr}/^{86}\text{Sr}$ values, whereas the fine fraction mainly contains clay minerals and micas, which are characterized by high $^{87}\text{Sr}/^{86}\text{Sr}$ ratios [Chen *et al.*, 2007; Colin *et al.*, 2006; Hu *et al.*, 2012; Innocent *et al.*, 2000; Meyer *et al.*, 2011]. We tested this idea by comparing Sr-Nd isotope compositions of the clay-sized silicate fraction of loess and river sediments with bulk samples from previous studies (Figure 6a). It is striking that the clay-sized fractions have higher $^{87}\text{Sr}/^{86}\text{Sr}$ values than the bulk samples, whereas the $\epsilon_{\text{Nd}(0)}$ values of the clay-sized fractions are similar to those of the bulk fractions despite some subtle variations. In most cases, sediment sorting makes the sediment grain-size changes significantly during their transport and disposition from source to sink [Lupker *et al.*, 2013]. Therefore, use of Pb and Sr isotopes for provenance work with bulk sediment samples should be undertaken with caution. Clearly, if isotopic composition is to be used to constrain sedimentary provenance then comparing the same grain-size fraction in both potential sources and sinks is more reliable than bulk samples.

In order to constrain how the composition of paleo-Yellow River sediments changed since the last glacial, we also analyzed samples from Core M7-6, which is located only 65 km away from the modern Yellow River mouth (Figure 1a). This can be regarded as an ideal location to record the history of the Yellow River over that time period. Despite of the fact that the Yellow River has changed the location of its river mouth frequently since the last glacial [Liu *et al.*, 2001; Liu *et al.*, 2009], the Yellow River could have delivered sediments to the delta in the Bohai Sea [Hu *et al.*, 2012] and even surrounding areas [Liu *et al.*, 2009] in the late last deglacial (13–10.4 ka BP) and Holocene (~ 7 –0 ka BP) [Liu *et al.*, 2001]. Therefore Core M7-6 could have received sediments from the Yellow River within a certain period of time (i.e., ~ 14.7 –11 ka BP and ~ 7 –0 ka BP) both in late last deglacial and Holocene, and can be used to investigate any discrepancy between these two periods. Furthermore, it has been suggested that about 90% of the Yellow River sediment load come

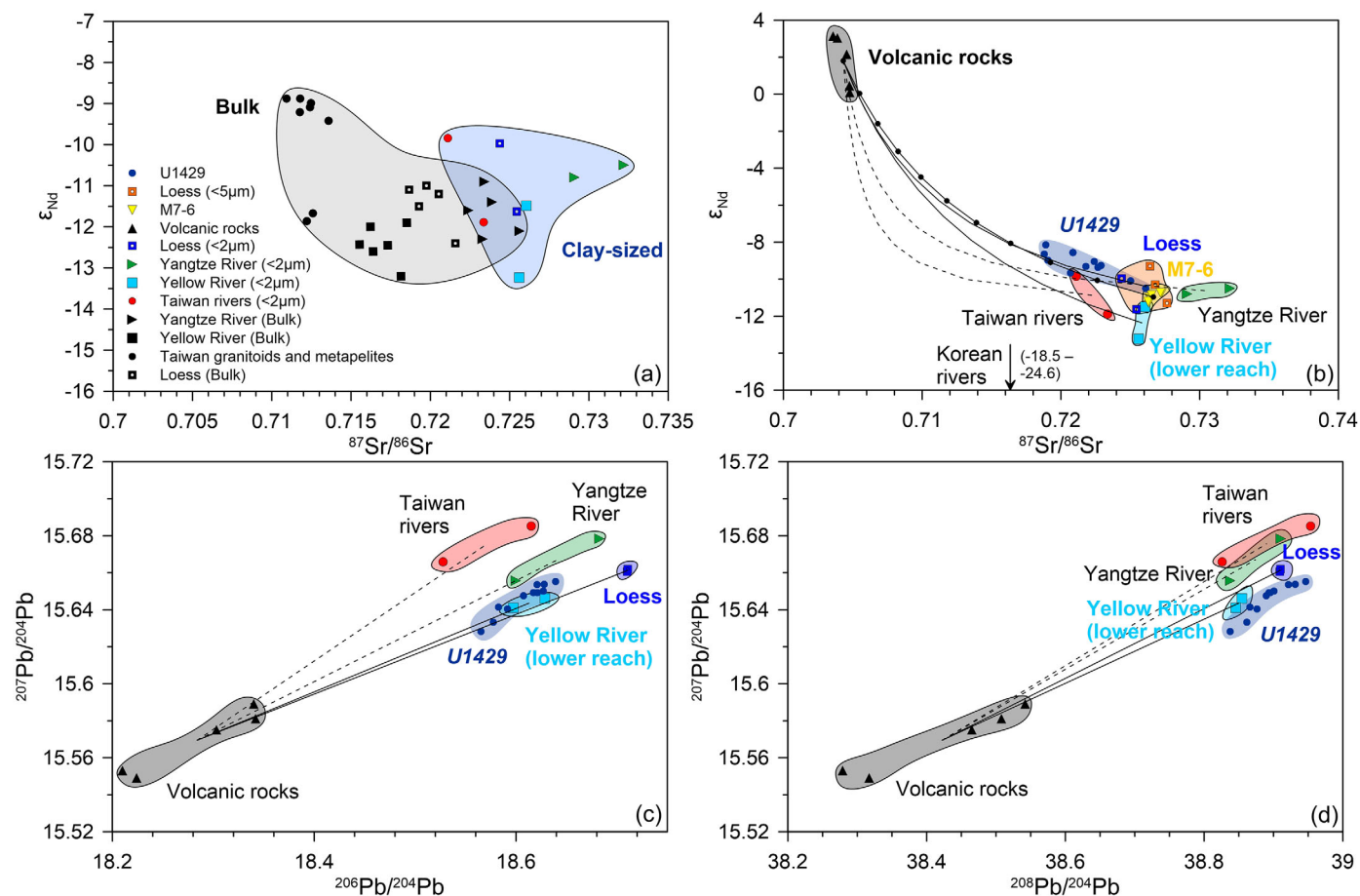


Figure 6. (a) Comparison of $^{86}Sr/^{87}Sr$ versus $\epsilon_{Nd(0)}$ between clay-sized particles (This study) and bulk (unsized) samples. Bulk samples data (average values) are shown in Table 4. (b) Discrimination plot of $^{86}Sr/^{87}Sr$ versus $\epsilon_{Nd(0)}$ in IODP Site U1429 clay-sized particles of sediments, in comparison with those of potential sources. Volcanic rocks data are from Hosono *et al.* [2003]. Loess isotope data of $<5\ \mu m$ particles are from Biscaye *et al.* [1997]. South Korean river $\epsilon_{Nd(0)}$ data (bulk samples) are from Lee *et al.* [2008]. The arrow shows the value of $\epsilon_{Nd(0)}$ (-18.5 to -24.6) of Korean river sediments. (c and d) Discrimination plot of Pb isotopes ($^{206}Pb/^{204}Pb$ versus $^{207}Pb/^{204}Pb$ and $^{208}Pb/^{204}Pb$ versus $^{207}Pb/^{204}Pb$) in IODP Site U1429 clay-sized sediments, in comparison with those of potential sources. Volcanic rocks data are from Hosono *et al.* [2003]. Sr, Nd, and Pb average concentrations (ppm) in the potential end-members are shown in Table 4.

from the middle and upper reaches, especially the Loess Plateau [Ren and Shi, 1986]. Consequently, changes in the channel of Yellow River in the lower reaches have little impact on the composition of sediments transported to the sea. Interestingly, we observed no major fluctuation in the $^{87}Sr/^{86}Sr$ (from 0.726281 to 0.727273) or $\epsilon_{Nd(0)}$ (from -11.3 to -10.7) of clay-sized samples from the late deglacial to Holocene. This contrasts with the large changes in $^{87}Sr/^{86}Sr$ (from 0.716389 to 0.723884) and $\epsilon_{Nd(0)}$ (from -14.5 to -11.9) of bulk silt samples of another sediment core in the Yellow River mouth, spanning the same time period [Hu *et al.*, 2012]. It is possible that sediments from different grain-size intervals could have different sources. According to the data of Hu *et al.* [2012], fine-grained particles with more positive $\epsilon_{Nd(0)}$ were mainly found during MIS 1 and 3, and interpreted as being supplied from the Loess Plateau. However, more negative values of $\epsilon_{Nd(0)}$ were in phase with deposition of coarse-grained sediments in MIS 2 and 4, which were attributed to the main source shifting from the Loess Plateau to the desert. Therefore, clay-sized sediments from Core M7-6 probably have a stable source in Loess Plateau since the last deglacial. Our data strongly suggest that the source of clay-sized Yellow River sediments remained stable since at least the late last deglacial.

To identify the provenance of sediments at IODP Site U1429, $^{87}Sr/^{86}Sr$ was plotted against $\epsilon_{Nd(0)}$. Furthermore Pb isotopes ($^{206}Pb/^{204}Pb$ versus $^{207}Pb/^{204}Pb$ and $^{208}Pb/^{204}Pb$ versus $^{207}Pb/^{204}Pb$) diagrams were plotted with data from IODP Site U1429 and potential sources including southern Kyushu volcanic rocks, Yellow River lower reaches and mouth (Core M7-6), loess, the Yangtze and Taiwanese rivers. The loess end-member represents sources in the Yellow River upper reaches (Figures 6b–6d). The very good

correspondence between Core M7-6 and loess samples indicates the stable sediments source of Yellow River clay-sized sediments since the last deglacial. Samples from IODP Site U1429 have more positive values of $\epsilon_{\text{Nd}(0)}$ than East Asian river sediments (Figure 6b), which requires an additional contribution from isotopically positive volcanic sources. In order to quantify this, mixing models of two end-members between a Kyushu end-member and each potential source were established. As shown in Figure 6b, most samples from IODP Site U1429 plot along the mixing lines of Kyushu-Core M7-6 and Kyushu-loess. The deviation between IODP Site U1429 samples and the Kyushu-Yellow River lower reaches mixing line is probably induced by the limited Yellow River lower reach samples that we analyzed. It is clear that the samples deviate from the Kyushu Island-Taiwan mixing line. For the Korean river end-member, the much more negative $\epsilon_{\text{Nd}(0)}$ (−18.5 to −24.6) compared to other potential source areas makes it impossible for the U1429 samples to plot along the Kyushu volcanic rock-Korean river mixing line. However, there are three samples that plot close to the Kyushu-Yangtze River mixing line.

On the $^{206}\text{Pb}/^{204}\text{Pb}$ versus $^{207}\text{Pb}/^{204}\text{Pb}$ diagram (Figure 6c), samples from IODP Site U1429 plot near the Yellow River lower reaches and are located on the Kyushu-loess and Kyushu-Yellow River mixing lines. Furthermore, the compositions could also reflect slight influence from the Yangtze River. However, if we consider the $^{208}\text{Pb}/^{204}\text{Pb}$ versus $^{207}\text{Pb}/^{204}\text{Pb}$ diagram (Figure 6d), all the samples from Site U1429 are close to the loess and Yellow River (lower reach), and show no similarity with the Yangtze or Taiwanese rivers. Because Yellow River sediments transported to the sea are potentially a mixture from the whole river drainage basin, we regard Core M7-6 from the Yellow River mouth as the most representative end-member of Yellow River flux. The isotope source tracing results suggest that clay-sized sediments at IODP Site U1429 are mainly derived from the Yellow River and Kyushu.

Based on the clay mineralogy and isotopic source tracing results, we propose the provenance of clay-sized sediments from IODP Site U1429 to be the Yellow River and Kyushu. However, our result is incompatible with previous models that Taiwan-derived sediments transported by the Kuroshio Current are a significant contribution to the northern Okinawa Trough since 7.3 ka BP based on evidence from clay minerals *Xu et al.* [2014] and Sr-Nd isotopes measured on bulk samples *Li et al.* [2015]. However, these earlier studies did not account for flux from Kyushu or the possibility of different sources for different grain-size fractions. Despite the fact that we exclude Taiwan as a significant source to the clay-sized sediments in the northern Okinawa Trough since 34 ka BP, this does not require that the Kuroshio Current has not flowed into the Okinawa Trough during the LGM. *Zheng et al.* [2014] and *Zheng et al.* [2016] argued that $\sim 11 \mu\text{m}$ Taiwan-derived sediments, not clay-sized ($< 2 \mu\text{m}$), were transported by the Kuroshio Current to the north. Accordingly, we argue that the contribution of Taiwan to the flux of clay-sized sediments is insignificant to this area. Furthermore, our study emphasizes an additional contribution from Kyushu.

4.2. Clay-Sized Sediment Flux From the Yellow River and Kyushu Island

Quantitative estimates of the contributions from each end-member sediment source through time are the key to understand the sediment transport mechanisms in the Okinawa Trough during the late Quaternary. Estimates of varying clay-sized particle fluxes from Kyushu and the Yellow River are based on isotope data from southern Kyushu volcanic rocks and Core M7-6 mixing models. It is reasonable to assume that the Kyushu end-member has been relatively stable since 34 ka BP, whereas changes in the Yellow River end-member since the last glacial period can be traced using isotope records from Core M7-6. Considering a stable Yellow River clay-sized sediment composition since the late last deglacial proposed by the Core M7-6, we here adopt the average Sr-Nd isotope values of the core since the last deglacial as the Yellow River end-member in order to calculate the relative supply of clay-sized particles. The results suggest that the Yellow River supplied approximately 75–95% of the clay-sized sediments to the study site during the late glacial and deglacial, and 71–86% in the Holocene. In contrast, the relative contribution from Kyushu clay-sized shows a reverse trend, with a contribution of 5–25% during the late glacial and deglacial, and 14–29% in the Holocene.

Yellow River and Kyushu-derived clay-sized sediments fluxes were determined by multiplying the terrigenous MAR by the weight percent value of each (Figures 7e and 7g). Clay-sized Yellow River sediments show higher MARs during the last glacial and deglacial (average $35.7 \text{ g/cm}^2/\text{ka}$) than the Holocene (average $11.2 \text{ g/cm}^2/\text{ka}$). For Kyushu, the clay-sized sediment MARs show strong fluctuations, with higher values before $\sim 23.5 \text{ ka BP}$ (average $7.7 \text{ g/cm}^2/\text{ka}$) and from ~ 14 to 10 ka BP (average $8.6 \text{ g/cm}^2/\text{ka}$), and lower

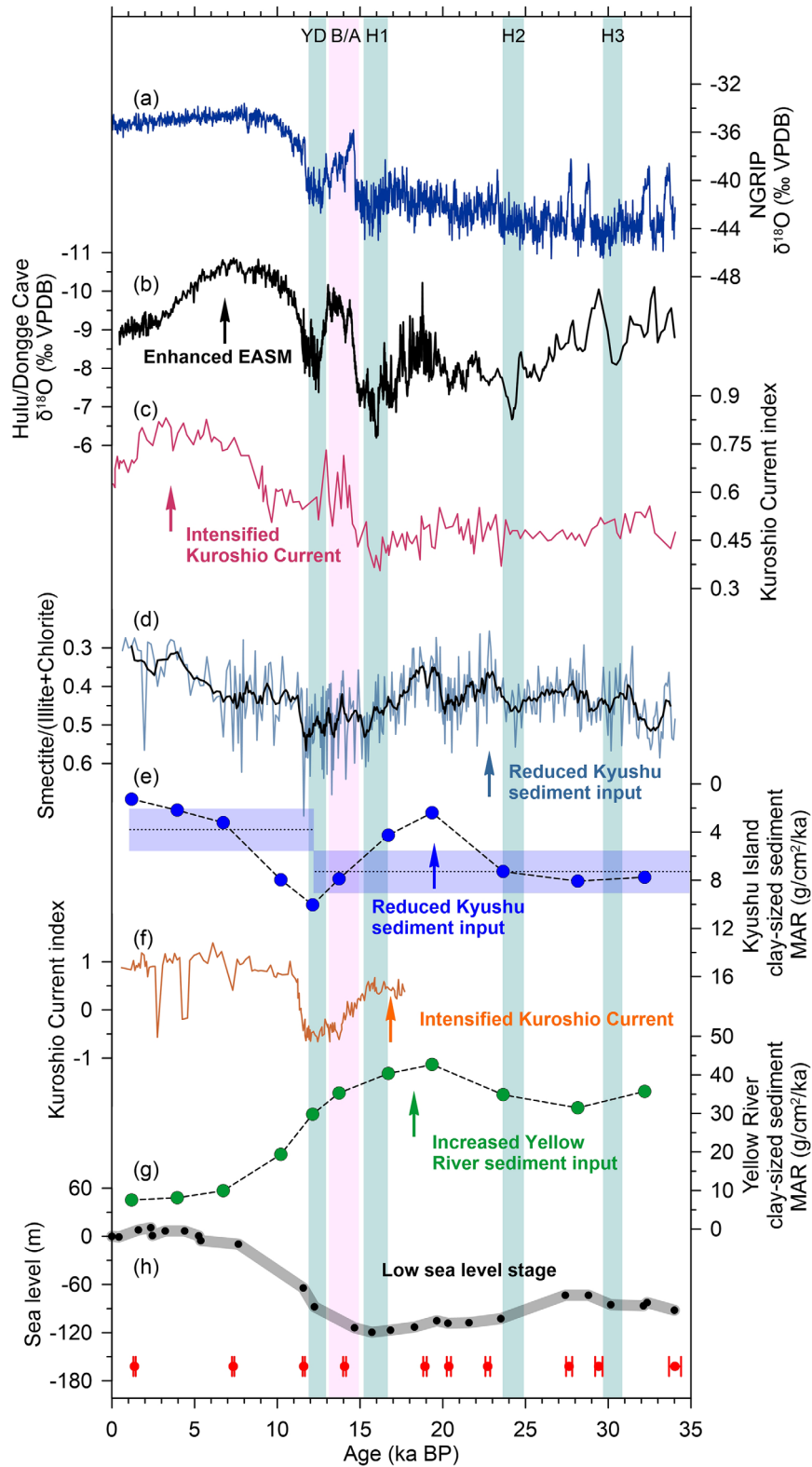


Figure 7. Variations of Yellow River clay-sized sediment MARs (g) compared with sea-level change (h) [Saito *et al.*, 1998], and Kyushu Island clay-sized sediment MAR (e) as well as clay mineral ratio smectite/(illite + chlorite) (d), compared with Kuroshio Current proxy (c) [Ijiri *et al.*, 2005], and (f) [Zheng *et al.*, 2016], $\delta^{18}\text{O}$ records Hulu and Dongge caves (b) [Dykoski *et al.*, 2005; Wang *et al.*, 2001] and the NGRIP (a) [Andersen *et al.*, 2004]. Shaded bars show intervals of Younger Dryas cooling (YD), Bølling-Ållerød warming (B/A), and Heinrich events (H1, H2 and H3). Red dots show 10 Accelerator Mass Spectrometry (AMS) ¹⁴C dates with an uncertainty of 2 σ .

values from ~ 23.5 to 14 ka BP (average $3.3 \text{ g/cm}^2/\text{ka}$), as well as from ~ 10 ka BP to the present-day (average $2.2 \text{ g/cm}^2/\text{ka}$).

4.3. Yellow River Sediment Transport and Sedimentation: Sea-Level Control

Clay-sized sediment fluxes from the Yellow River display anticorrelation with sea-level change since 34 ka BP (Figures 7g and 7h). The higher (lower) flux of Yellow River-derived clay-sized sediments occurred during low (high) sea-level stages, suggesting a sea-level control on sedimentation. During the last glacial and early deglacial period, the sea-level was about 80–120 m lower than today on the East China Sea shelf [Saito *et al.*, 1998]. The prominent sea-level fall led to the progradation of the coastline and exposure of the East China Sea shelf. In recent years, paleo-Yellow River channels have been found on the Yellow Sea shelf and northern East China Sea shelf [Li *et al.*, 1991; Jian Liu *et al.*, 2010] (Figure 8a). As a result, the paleo-Yellow River mouth moved to the shelf edge and was positioned close to the northern Okinawa Trough (Figure 8a), favoring large fluvial discharge or even direct input of detrital sediments from the paleo-Yellow River to the study area. This hypothesis is supported by the 4–5 times higher linear sedimentation rate and Yellow River clay-sized flux at IODP Site U1429 during the last glacial and deglacial compared to the Holocene (Figure 3). The Kuroshio Current may have remained in the Okinawa Trough and could have influenced the northern Okinawa Trough during the LGM [Ijiri *et al.*, 2005; Lee *et al.*, 2013]. However, low sea-level during the LGM resulted in a 43% reduction in Kuroshio Current inflow [Kao *et al.*, 2006]. If so sedimentation in the northern Okinawa Trough would be expected to be dominated by direct input from the paleo-Yellow River on the exposed shelf during the low sea-level stages rather than a significantly weakened Kuroshio Current. Along with the sea-level rise and retreated paleo-Yellow River mouth since about 15 ka BP, the Yellow River sediment input to the northern Okinawa Trough reduced gradually. Besides, the “blocking effects” of strengthened Kuroshio Current since about 15 ka BP (Figure 7) and occurrence of the Tsushima Warm Current at ~ 11 ka BP [Oba *et al.*, 1991; Yokoyama *et al.*, 2006] could also account for the reduced Yellow River sediment supply during the last deglacial.

Previous studies suggested that the Yellow River mouth gradually retreated with rising sea-level and reached its present position at about 8.5 ka BP [Saito *et al.*, 2000]. The pattern of modern oceanic circulation in the East China Sea was established at about 7.5–6.0 ka BP [Ujiie *et al.*, 1991] (Figure 8b). Since this time, sedimentation in the Okinawa Trough was influenced by the circulation system in the East China Sea. Yellow River material has mostly been deposited near the modern river mouth and around the Shandong Peninsula, with fine-grained particles transported southward along the coast by the Yellow Sea Coastal Current [Milliman *et al.*, 1989]. Moderate Resolution Imaging Spectroradiometer (MODIS) satellite observations suggest that Yellow River suspended particles reaching the northern Okinawa Trough originate mainly from the old Yellow River mouth by the cross-shelf current [Yuan *et al.*, 2008]. Previous studies argued that the Kuroshio Current strengthened since the early Holocene [Dou *et al.*, 2012; Zheng *et al.*, 2016], and the Kuroshio Current “water barrier” could reduce the suspended sediments transport from the East China Sea to the Okinawa Trough during high sea-level stages [Dou *et al.*, 2010b; Guo *et al.*, 2001; Xu *et al.*, 2014; Zheng *et al.*, 2016]. Because of the longer distance from the Yellow River mouth to the study area with rising sea-level and accounting for the blocking effect of the Kuroshio Current branches or the “water barrier” (Figure 8b), the fluxes of Yellow River-derived materials into the northern Okinawa Trough largely decreased during the late deglacial and Holocene, consistent with a dominant influence from sea-level.

4.4. Kyushu Sediment Transport and Sedimentation: Ocean Current Modulation

The study site is located about 100 km west of Kyushu (Figure 1a). The continental shelf along western Kyushu is very narrow (< 50 km). In comparison with the wide and flat shelves (~ 600 km) of the East China Sea, the effects of sea-level variation on fluvial input from Kyushu to the study site are expected to be negligible. As a result the clay-sized sediment input from Kyushu to the northern Okinawa Trough should be mainly regulated by monsoon precipitation-driven weathering and erosion onshore Kyushu and ocean current transport in the marine environment. In any case, flocculation of clay-sized sediments and local ocean dynamic processes such as wave activities, tidal currents, and other local current circulations in the Kyushu offshore area would also have the potential to regulate clay-sized sediment input and deposition.

As smectite and illite (chlorite) at the study site primarily originated from Kyushu and the Yellow River, respectively, we use the ratio of smectite/(illite + chlorite) at IODP Site U1429 as a proxy of changing

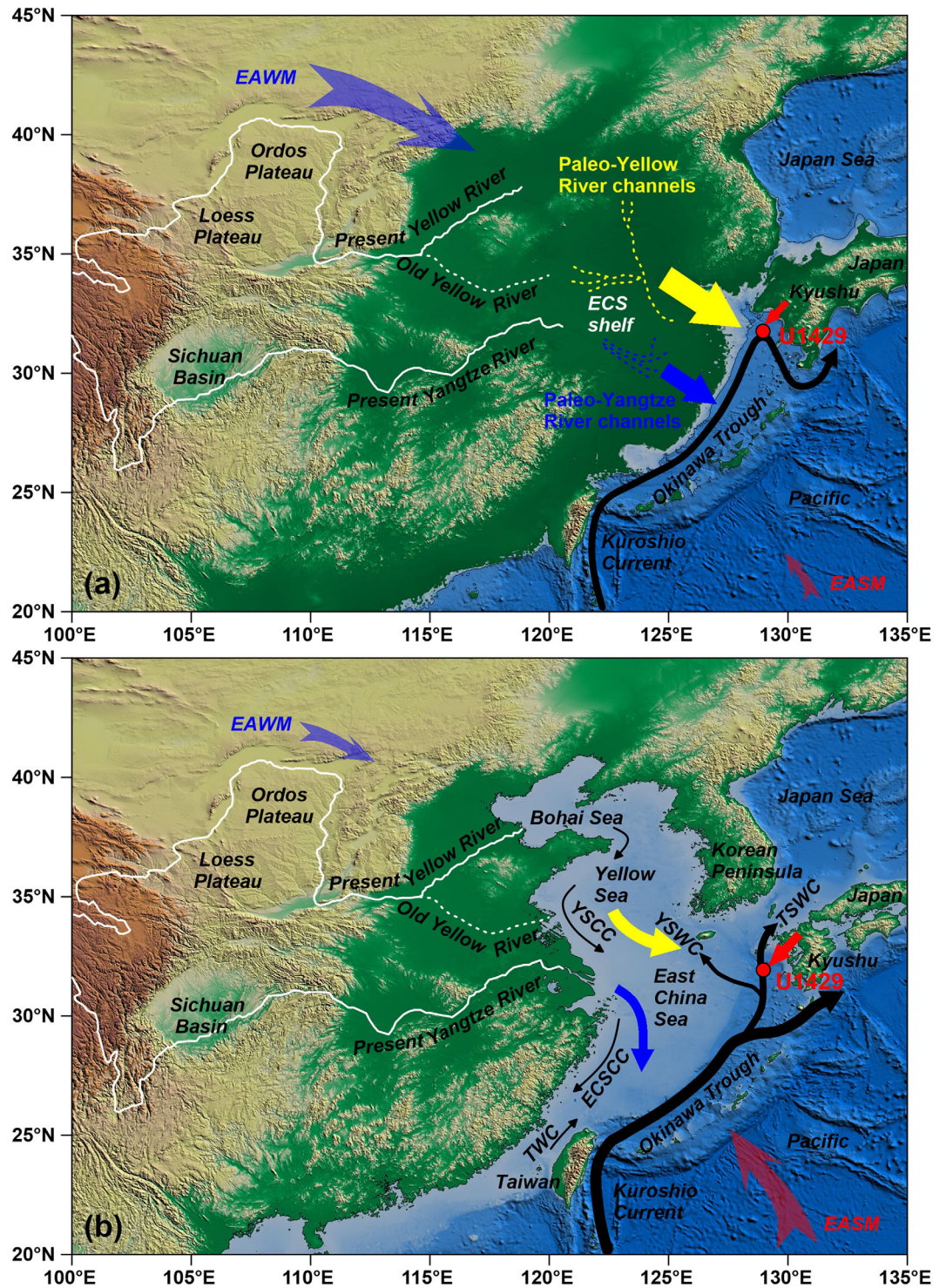


Figure 8. Map showing the sea-level change, ocean current evolution of East China Sea, and detrital sediments supply to IODP Site U1429 in the northern Okinawa Trough in (a) LGM and (b) present. Old Yellow River (white dash line) is shown from *Liu et al.* [2001]. The paleo-Yellow River valleys (yellow dash line) on the Yellow Sea/East China Sea shelves are from *Li et al.* [1991] and *Jian Liu et al.* [2010], and the paleo-Yangtze River valleys (blue dash line) on the East China Sea shelf are from *Li et al.* [2005]. The Kuroshio Current (black arrow line) during the LGM is modified from *[Lee et al., 2013]*. The circulation pattern (black arrow line) in the East China Sea and adjacent areas at present are from *Yuan et al.* [2008]. The Yellow River, Yangtze River, and Kyushu Island sediments inputs are shown by yellow, blue, and red arrows, respectively. The East Asian summer and winter monsoon are shown by red and blue translucent arrows, respectively.

strength of clay-sized fluvial input from Kyushu relative to the Yellow River. This hypothesis is supported by the consistent variation of smectite/(illite + chlorite) ratio and Sr-Nd isotopes-derived sediments fluxes from Kyushu since 34 ka BP (Figures 7d and 7e).

Grain-size of clay minerals has been regarded as the dominant controlling factor for the clay-sized sediment flocculation in the marine environment [Gibbs, 1977]. Illite and chlorite are larger (0.4–60 μm), with kaolinite second (0.4–10 μm) and smectite finest (<1 μm). As a result, the illite, chlorite, and kaolinite flocculate in preference to the smectite. Smectite can be transported more easily further offshore. Flocculation induced by grain-size does not have a significant impact on Kyushu-derived clay-sized sediments input to the northern Okinawa Trough. Zhang *et al.* [1995] suggested that salinity also controls clay-sized sediment flocculation. In the Yangtze River estuary, the illite and kaolinite flocculate and deposit in a lower salinity environment (9×10^{-3} – 13×10^{-3}), whereas smectite tends to flocculate in a relatively higher salinity environment (19×10^{-3} – 24×10^{-3}). As a result, a strengthened Kuroshio Current with high salinity water should promote smectite flocculation, and thus a higher content at the study site during the Holocene than during the late last glacial and deglacial. However, smectite/(illite + chlorite) values show more smectite delivery to the northern Okinawa Trough from Kyushu during the last glacial and deglacial than during the Holocene (Figure 7d). Therefore, flocculation induced by salinity does not control sedimentation of clay-sized sediment input from Kyushu to the northern Okinawa Trough.

Local ocean dynamic processes mainly regulate the sediment transport and deposition in the offshore of southern Kyushu, especially in Ariake Bay [Makino, 1994]. However, the study site is located on the western slope of the northern Okinawa Trough, about 100 km southwest of Kyushu. Thus the influence of such local dynamic processes should be slight. Furthermore, dynamic processes are short-time-scale activities. Even when local ocean dynamics are closely related to long-term climate conditions, they have been considered insignificant and have not been discussed when considering terrigenous sediment transport and deposition in the marine environment over millennial or orbital scales [Diekmann *et al.*, 2008; Hu *et al.*, 2013; Wan *et al.*, 2015]. Local ocean dynamics are not critical in controlling clay-sized sediment input and deposition at the study site on the study time scale.

In general, both the smectite/(illite + chlorite) and Kyushu clay-sized sediment MAR suggest that Kyushu supplied more clay-sized terrigenous sediments to the northern Okinawa Trough during the last glacial and deglacial than the Holocene (Figures 7d and 7e). However, $\delta^{18}\text{O}$ records from Hulu and Dongge caves indicate a stronger East Asian summer monsoon during the Holocene [Dykoski *et al.*, 2005; Wang *et al.*, 2001] (Figure 7b). This contradicts with the observations that stronger East Asian summer monsoon precipitation would be expected to enhance chemical weathering and physical erosion in subtropical and tropical East Asia [Clift *et al.*, 2008; Colin *et al.*, 2010; Hu *et al.*, 2013; Wan *et al.*, 2015]. We infer that East Asian summer monsoon precipitation is also not the main control over fine-grained sediment input from Kyushu on the glacial-interglacial time scale.

After eliminating the factors discussed above, the effect of the Kuroshio Current and its branch (Tsushima Warm Current) on clay-sized sediment transport would seem to be important. The main axis of the Kuroshio Current enters the Okinawa Trough northeast of Taiwan with a maximum speed of 100 cm/s and a width of 100 km [Liang *et al.*, 2003]. The current flows northeastward along the outer edge of the East China Sea shelf, and divides into three branches, Kuroshio extension, Tsushima Warm Current, and Yellow Sea Warm Current, which flow along the southern coast of Kyushu (Figure 1a). It has been proposed that the Kuroshio Current still flowed across the Okinawa Trough during the late last glacial and deglacial, and induced upwelling in the northern Okinawa Trough as the current climbed the continental slope [Jjiri *et al.*, 2005; Li *et al.*, 2007]. The generation of upwelling induced by the bathymetry is mainly driven by the water mass which induces a vertical velocity component when it encounters the rising slope [Li and Kong, 1988]. As a result, such upwelling suggests the impact of the Kuroshio Current onto the slope of the northern Okinawa Trough. At present day, the “water barrier” of Kuroshio Current has been regarded as an important factor obstructing the suspended matter from the East China Sea shelf into the deep trough [Yang *et al.*, 1992]. The “water barrier” prevails during summer due to strong Kuroshio Current climbing water and weakens during winter when East Asian winter monsoon strengthens, resulting in a different sediment transport pattern, i.e., summer storage and winter export of sediments on the ECS shelf [Yang *et al.*, 1992; Zheng *et al.*, 2016].

According to these facts, it is very likely that the Kuroshio Current could also obstruct Kyushu Island derived clay-sized sediments input to the study site during the last glacial and deglacial. In contrast, it has been suggested that the first major intrusion of the Tsushima Warm Current in the Japan Sea at ~ 11.5 – 11 ka BP [Oba *et al.*, 1991; Tada *et al.*, 1999; Yokoyama *et al.*, 2006]. Therefore the influence of the Tsushima Warm Current on the study areas probably started at this time. Oceanographic observation using drogued drifters provides clear evidence that the Tsushima Warm Current flows along the western slope of northern Okinawa Trough near the study site, and also influences the southwest of Kyushu Island [Lie *et al.*, 1998]. Therefore, the Tsushima Warm Current could exert similar blocking effect to regulate the Kyushu Island clay-sized sediment input to the Okinawa Trough since about 11 ka BP. Such an interpretation is supported by the distribution of surface sediments types south of Kyushu. Silt-clay sediments are distributed in the nearshore area, while medium-coarse sand sediments are distributed offshore [Li and Chang, 2009]. It has also been proposed the volcanic materials from the Japanese Arc are hard to transport to the west due to the Kuroshio Current “blocking effect,” thus resulting in a decrease trend of volcanic mineral concentrations between the northern Okinawa Trough and the East China Sea shelf [Li and Chang, 2009]. Accordingly, Kyushu-derived sediments could be very likely influenced by the Kuroshio Current during the last glacial and deglacial and by Tsushima Warm Current since about 11 ka BP, which prevent clay-sized sediment input to the study site. In this case, changes in current intensity could regulate the Kyushu Island derived clay-sized sediments input to the northern Okinawa Trough.

Interestingly, the smectite/(illite + chlorite) and Kyushu clay-sized sediment MAR show coherent variation with published Kuroshio Current indexes based on the planktonic foraminiferal assemblage in the northern Okinawa Trough [Jjiri *et al.*, 2005] and grain-size V-PCA analyses proposed by Zheng *et al.* [2016] before ~ 11 ka BP (Figures 7c and 7f). On millennial-scale, the Kyushu-derived clay-sized sediment input increased during Heinrich events H3 (~ 31 – 30 ka BP), H2 (~ 25 – 24 ka BP), and H1 (~ 16.5 – 15.5 ka BP), the Younger Dryas (~ 13 – 12 ka BP), probably suggesting a weakened Kuroshio Current intensity during these periods. The rapid decreased ratio of smectite/(illite + chlorite) during ~ 12 – 11 ka BP suggesting the strengthening of the role of “blocking effect,” which probably related to the occurrence of Tsushima Warm Current [Oba *et al.*, 1991; Yokoyama *et al.*, 2006]. The relatively stable ratio of smectite/(illite + chlorite) during ~ 11 – 7 ka BP probably suggesting a constant Tsushima Warm Current, which then strengthened since ~ 7 ka BP, excepting some fluctuations around 4–3 ka BP (Figure 7). Future work of observation and simulation is needed to further constrain the sedimentary dynamic process of Kyushu fine-grained particles input to the northern Okinawa Trough, and find the reliable proxies of Kuroshio Current and/or Tsushima Warm Current, which will provide a new perspective on the evolution of west boundary current in East Asian marginal seas in the geological past.

5. Conclusions

High-resolution terrigenous clay minerals and Sr-Nd-Pb isotopes analyses of clay-sized sediment were used to reconstruct terrigenous provenance variations in the northern Okinawa Trough, and establish the relation between fine-grained sediment input, sea-level change, and Kuroshio Current/Tsushima Warm Current evolution.

Provenance proxies indicated that clay-sized sediments in the northern Okinawa Trough were mainly derived from the Yellow River and Kyushu. Clay-sized sediment input from the Yellow River to the northern Okinawa Trough was strongly influenced by sea-level since 34 ka BP. During low sea-level, the paleo-Yellow River mouth was positioned significantly closer to the northern Okinawa Trough, favoring large fluvial discharge or even direct input of detrital sediments to the study area. With the sea-level rise since the late deglacial, the Yellow River mouth retreated and the blocking effect of Kuroshio Current branches strengthened gradually, resulting in a significant reduction in clay-sized sediment flux from the Yellow River to the northern Okinawa Trough. Clay-sized sediment input from Kyushu to the northern Okinawa Trough was mainly controlled by Kuroshio Current and Tsushima Warm Current intensity, with increased input in phase with weakened Kuroshio Current/Tsushima Warm Current. During ~ 34 – 11 ka BP, the Kyushu fine-grained sediment input was mainly controlled by the Kuroshio Current. Since ~ 11 ka BP, the developed Tsushima Warm Current began influence the Kyushu fine-grained sediment input to the northern Okinawa Trough.

Acknowledgments

The original data of this study are available in supporting information Table S1. We acknowledge the Integrated Ocean Drilling Program and the scientific party and technicians of IODP Expedition 346 for recovering the samples. We thank the editor Yusuke Yokoyama and reviewer Andrea Erhardt and another anonymous reviewer for their constructive comments. This work was supported by the National Natural Science Foundation of China (41576034, 41622603, U1606401), National Program on Global Change and Air-Sea Interaction (GASI-GEOGE-03), Strategic Science Project of Chinese Academy of Sciences (CAS) (XDA11030104), Innovation Project of Qingdao National Laboratory (2016ASKJ13) and CAS Interdisciplinary Innovation Team.

References

- Andersen, K. K., et al. (2004), High-resolution record of Northern Hemisphere climate extending into the last interglacial period, *Nature*, *431*(7005), 147–151.
- Aoki, S., and K. Oinuma (1974), Clay mineral compositions in recent marine sediments around Nansei-Kyoto islands, south of Kyushu, Japan, *J. Geol. Soc. Jpn.*, *80*, 57–63.
- Arakawa, Y., M. Kurosawa, K. Takahashi, Y. Kobayashi, M. Tsukui, and H. Amakawa (1998), Sr-Nd isotopic and chemical characteristics of the silicic magma reservoir of the Aira pyroclastic eruption, southern Kyushu, Japan, *J. Volcanol. Geotherm. Res.*, *80*(3), 179–194.
- Aumento, F., W. Mitchell, and M. Fratta (1976), Interaction between seawater and oceanic layer two as a function of time and depth, 1. Field evidence, *Can. Mineral.*, *14*, 269–290.
- Bentahila, Y., D. Ben Othman, and J. M. Luck (2008), Strontium, lead and zinc isotopes in marine cores as tracers of sedimentary provenance: A case study around Taiwan Orogen, *Chem. Geol.*, *248*(1–2), 62–82.
- Biscaye, P. E. (1965), Mineralogy and sedimentation of recent deep-sea clay in the Atlantic Ocean and adjacent seas and oceans, *Geol. Soc. Am. Bull.*, *76*(7), 803–832.
- Biscaye, P. E., F. Grousset, M. Revel, S. Van der Gaast, G. Zielinski, A. Vaars, and G. Kukla (1997), Asian provenance of glacial dust (stage 2) in the Greenland Ice Sheet Project 2 ice core, Summit, Greenland, *J. Geophys. Res.*, *102*(C12), 26,765–26,781.
- Bluth, G. J., and L. R. Kump (1994), Lithologic and climatologic controls of river chemistry, *Geochim. Cosmochim. Acta*, *58*(10), 2341–2359.
- Chamley, H. (1989), *Clay Sedimentology*, pp. 623, Springer, Berlin.
- Chang, F., T. Li, Z. Xiong, and Z. Xu (2015), Evidence for sea level and monsoonally driven variations in terrigenous input to the northern East China Sea during the last 24.3 ka, *Paleoceanography*, *30*(6), 642–658.
- Chen, J., G. Li, J. Yang, W. Rao, H. Lu, W. Balsam, Y. Sun, and J. Ji (2007), Nd and Sr isotopic characteristics of Chinese deserts: Implications for the provenances of Asian dust, *Geochim. Cosmochim. Acta*, *71*(15), 3904–3914.
- Chen, P. (1973), Clay minerals distribution in the sea-bottom sediments neighboring Taiwan Island and northern South China Sea, *Acta Oceanogr. Taiwan*, *3*, 25–64.
- Clift, P. D. (2016), Assessing effective provenance methods for fluvial sediment in the South China Sea, *Geol. Soc. Spec. Publ.*, *429*(1), 9–29.
- Clift, P. D., et al. (2008), Holocene erosion of the Lesser Himalaya triggered by intensified summer monsoon, *Geology*, *36*(1), 79–82.
- Clift, P. D., S. Wan, and J. Blusztajn (2014), Reconstructing chemical weathering, physical erosion and monsoon intensity since 25 Ma in the northern South China Sea: A review of competing proxies, *Earth Sci. Rev.*, *130*, 86–102.
- Colin, C., L. Turpin, D. Blamart, N. Frank, C. Kissel, and S. Duchamp (2006), Evolution of weathering patterns in the Indo-Burman Ranges over the last 280 kyr: Effects of sediment provenance on $^{87}\text{Sr}/^{86}\text{Sr}$ ratios tracer, *Geochem. Geophys. Geosyst.*, *7*, Q03007, doi:10.1029/2005GC000962.
- Colin, C., G. Siani, M.-A. Sicre, and Z. Liu (2010), Impact of the East Asian monsoon rainfall changes on the erosion of the Mekong River basin over the past 25,000 yr, *Mar. Geol.*, *271*(1), 84–92.
- Dane, J. H., C. Topp, G. S. Campbell, R. Horton, W. A. Jury, D. R. Nielsen, H. M. van Es, P. J. Wierenga, and G. C. Topp (2002), *Part 4. Physical Methods, Methods of Soil Analysis*, Soil Sci. Soc. of Am., Madison, Wis.
- Dessert, C., B. Dupré, L. M. François, J. Schott, J. Gaillardet, G. Chakrapani, and S. Bajpai (2001), Erosion of Deccan Traps determined by river geochemistry: Impact on the global climate and the $^{87}\text{Sr}/^{86}\text{Sr}$ ratio of seawater, *Earth Planet. Sci. Lett.*, *188*(3), 459–474.
- Diekmann, B., J. Hofmann, R. Henrich, D. K. Fütterer, U. Röhl, and K. Y. Wei (2008), Detrital sediment supply in the southern Okinawa Trough and its relation to sea-level and Kuroshio dynamics during the late Quaternary, *Mar. Geol.*, *255*(1–2), 83–95.
- Dou, Y., S. Yang, Z. Liu, P. D. Clift, X. Shi, H. Yu, and S. Berne (2010a), Provenance discrimination of siliciclastic sediments in the middle Okinawa Trough since 30 ka: Constraints from rare earth element compositions, *Mar. Geol.*, *275*(1–4), 212–220.
- Dou, Y., S. Yang, Z. Liu, P. D. Clift, H. Yu, S. Berne, and X. Shi (2010b), Clay mineral evolution in the central Okinawa Trough since 28 ka: Implications for sediment provenance and paleoenvironmental change, *Palaeogeogr. Palaeoclimatol. Palaeoecol.*, *288*(1–4), 108–117.
- Dou, Y., S. Yang, Z. Liu, X. Shi, J. Li, H. Yu, and S. Berne (2012), Sr–Nd isotopic constraints on terrigenous sediment provenances and Kuroshio Current variability in the Okinawa Trough during the late Quaternary, *Palaeogeogr. Palaeoclimatol. Palaeoecol.*, *365*–366, 38–47.
- Dykoski, C. A., R. L. Edwards, H. Cheng, D. Yuan, Y. Cai, M. Zhang, Y. Lin, J. Qing, Z. An, and J. Revenaugh (2005), A high-resolution, absolute-dated Holocene and deglacial Asian monsoon record from Dongge Cave, China, *Earth Planet. Sci. Lett.*, *233*(1), 71–86.
- Ehrmann, W. (1998), Implications of late Eocene to early Miocene clay mineral assemblages in McMurdo Sound (Ross Sea, Antarctica) on paleoclimate and ice dynamics, *Palaeogeogr. Palaeoclimatol. Palaeoecol.*, *139*(3), 213–231.
- Erel, Y., Y. Harlavan, and J. D. Blum (1994), Lead isotope systematics of granitoid weathering, *Geochim. Cosmochim. Acta*, *58*(23), 5299–5306.
- Esquevin, J. (1969), Influence de la composition chimique des illites sur leur cristallinité, *Bull. Centre Rech. Pau-SNPA*, *3*(1), 147–153.
- Fan, D., Z. Yang, D. Mao, and Z. Guo (2001), Clay minerals and geochemistry of the sediments from the Yangtze and Yellow Rivers, *Mar. Geol. Quat. Geol.*, *21*(4), 7–12.
- Flemming, B. (1981), Factors controlling shelf sediment dispersal along the southeast African continental margin, *Mar. Geol.*, *42*(1–4), 259–277.
- Gibbs, R. J. (1977), Clay mineral segregation in the marine environment, *J. Sediment. Res.*, *47*(1), 237–243.
- Guo, Z., Z. Yang, K. Lei, L. Gao, and Y. Qu (2001), The distribution and composition of suspended matters and their influencing factors in the central-southern area of Okinawa Trough and its adjacent shelf sea, *Acta Oceanol. Sin.*, *23*(1), 66–72.
- He, M., H. Zheng, X. Huang, J. Jia, and L. Li (2013), Yangtze River sediments from source to sink traced with clay mineralogy, *J. Asian Earth Sci.*, *69*, 60–69.
- Hosono, T., T. Nakano, and H. Murakami (2003), Sr–Nd–Pb isotopic compositions of volcanic rocks around the Hishikari gold deposit, southwest Japan: Implications for the contribution of a felsic lower crust, *Chem. Geol.*, *201*(1), 19–36.
- Hu, B., G. Li, J. Li, J. Bi, J. Zhao, and R. Bu (2012), Provenance and climate change inferred from Sr–Nd–Pb isotopes of late Quaternary sediments in the Huanghe (Yellow River) Delta, China, *Quat. Res.*, *78*(3), 561–571.
- Hu, D., P. D. Clift, P. Böning, R. Hannigan, S. Hillier, J. Blusztajn, S. Wan, and D. Q. Fuller (2013), Holocene evolution in weathering and erosion patterns in the Pearl River delta, *Geochem. Geophys. Geosyst.*, *14*, 2349–2368, doi:10.1002/ggge.20166.
- Hu, D., L. Wu, W. Cai, A. S. Gupta, A. Ganachaud, B. Qiu, A. L. Gordon, X. Lin, Z. Chen, and S. Hu (2015), Pacific western boundary currents and their roles in climate, *Nature*, *522*(7556), 299–308.
- Huang, J., A. Li, and S. Wan (2011), Sensitive grain-size records of Holocene East Asian summer monsoon in sediments of northern South China Sea slope, *Quat. Res.*, *75*(3), 734–744.
- Ijiri, A., L. Wang, T. Oba, H. Kawahata, C.-Y. Huang, and C.-Y. Huang (2005), Paleoenvironmental changes in the northern area of the East China Sea during the past 42,000 years, *Palaeogeogr. Palaeoclimatol. Palaeoecol.*, *219*(3–4), 239–261.

- Innocent, C., N. Fagel, and C. Hillaire-Marcel (2000), Sm-Nd isotope systematics in deep-sea sediments: Clay-size versus coarser fractions, *Mar. Geol.*, *168*(1), 79–87.
- Jacobsen, S. B., and G. Wasserburg (1980), Sm-Nd isotopic evolution of chondrites, *Earth Planet. Sci. Lett.*, *50*(1), 139–155.
- Jian, Z., Y. Saito, P. Wang, B. Li, and R. Chen (1998), Shifts of the Kuroshio axis over the last 20 000 years, *Chin. Sci. Bull.*, *43*(12), 1053–1056.
- Jiang, H., P. Wang, J. Thompson, Z. Ding, and Y. Lu (2009), Last glacial climate instability documented by coarse-grained sediments within the loess sequence, at Fanjiaping, Lanzhou, China, *Quat. Res.*, *72*(1), 91–102.
- Kao, S. J., C.-R. Wu, Y.-C. Hsin, and M. Dai (2006), Effects of sea level change on the upstream Kuroshio Current through the Okinawa Trough, *Geophys. Res. Lett.*, *33*, L16604, doi:10.1029/2006GL026822.
- Kawahata, H., and H. Ohshima (2004), Vegetation and environmental record in the northern East China Sea during the late Pleistocene, *Global Planet. Change*, *41*(3), 251–273.
- Kim, D. C. (1979), Recent clay minerals of the Yeongsan estuary and the adjacent continental shelf, MS thesis, Dep. of Oceanogr., the Grad. Sch., Seoul Natl. Univ., Korea.
- Kitagawa, H., H. Fukuzawa, T. Nakamura, M. Okamura, K. Takemura, A. Hayashida, and Y. Yasuda (1995), AMS ^{14}C dating of varved sediments from Lake Suigetsu, central Japan and atmospheric ^{14}C change during the late Pleistocene, *Radiocarbon*, *37*(2), 371–378.
- Kubota, Y., K. Kimoto, R. Tada, H. Oda, Y. Yokoyama, and H. Matsuzaki (2010), Variations of East Asian summer monsoon since the last deglaciation based on Mg/Ca and oxygen isotope of planktic foraminifera in the northern East China Sea, *Paleoceanography*, *25*, PA4205, 10.1029/2009PA001891.
- Lan, C.-Y., T. Lee, B.-M. Jahn, and T.-F. Yui (1995), Taiwan as a witness of repeated mantle inputs—Sr-Nd-O isotopic geochemistry of Taiwan granitoids and metapelites, *Chem. Geol.*, *124*(3), 287–303.
- Lee, K. E., H. J. Lee, J. H. Park, Y. P. Chang, K. Ikehara, T. Itaki, and H. K. Kwon (2013), Stability of the Kuroshio path with respect to glacial sea level lowering, *Geophys. Res. Lett.*, *40*, 392–396, doi:10.1012/GRL.50102.
- Lee, S., J. Kim, D. Yang, and J. Kim (2008), Rare earth element geochemistry and Nd isotope composition of stream sediments, south Han River drainage basin, Korea, *Quat. Int.*, *176*, 121–134.
- Li, C., X. Shi, S. Kao, M. Chen, Y. Liu, X. Fang, H. Lü, J. Zou, S. Liu, and S. Qiao (2012), Clay mineral composition and their sources for the fluvial sediments of Taiwanese rivers, *Chin. Sci. Bull.*, *57*(6), 673–681.
- Li, F., and X. Kong (1988), A preliminary study on the relation of the offshore upwelling to bottom topography [in Chinese with English abstract], *J. Oceanogr. Huanghai Bohai Seas*, *6*(2), 39–46.
- Li, F., J. Yu, X. Jiang, Q. Du, and H. Song (1991), Study on buried paleo-channel system in the South Yellow Sea [in Chinese with English abstract], *Oceanol. Limnol. Sin.*, *22*(6), 501–508.
- Li, G. (1990), Composition, distribution and geology significance of clay mineral in surface sediments in China sea, *Acta Oceanol. Sin.*, *12*, 470–479.
- Li, G., Y. Liu, Z. Yang, S. Yue, W. Yang, and X. Han (2005), Ancient Changjiang channel system in the East China Sea continental shelf during the last glaciation, *Sci. China Ser. D*, *48*(11), 1972–1978.
- Li, T., and F. Chang (2009), *Paleoceanography in the Okinawa Trough [In Chinese]*, Ocean Press, Beijing.
- Li, T., R. Sun, D. Zhang, Z. Liu, Q. Li, and B. Jiang (2007), Evolution and variation of the Tsushima warm current during the late Quaternary: Evidence from planktonic foraminifera, oxygen and carbon isotopes, *Sci. China Ser. D*, *50*(5), 725–735.
- Li, T., Z. Xu, D. Lim, F. Chang, S. Wan, H. Jung, and J. Choi (2015), Sr-Nd isotopic constraints on detrital sediment provenance and paleoenvironmental change in the northern Okinawa Trough during the late Quaternary, *Palaeogeogr. Palaeoclimatol. Palaeoecol.*, *430*, 74–84.
- Liang, W.-D., T. Tang, Y. Yang, M. Ko, and W.-S. Chuang (2003), Upper-ocean currents around Taiwan, *Deep Sea Res., Part II*, *50*(6), 1085–1105.
- Lie, H. J., and C. H. Cho (2002), Recent advances in understanding the circulation and hydrography of the East China Sea, *Fish. Oceanogr.*, *11*(6), 318–328.
- Lie, H. J., C. H. Cho, J. H. Lee (1998), Separation of the Kuroshio water and its penetration onto the continental shelf west of Kyushu, *J. Geophys. Res.*, *103*(C2), 2963–2976.
- Liu, J., J. Milliman, and S. Gao (2001), The Shandong mud wedge and post-glacial sediment accumulation in the Yellow Sea, *Geo Mar. Lett.*, *21*(4), 212–218.
- Liu, J., Y. Saito, H. Wang, L. Zhou, and Z. Yang (2009), Stratigraphic development during the Late Pleistocene and Holocene offshore of the Yellow River delta, Bohai Sea, *J. Asian Earth Sci.*, *36*(4), 318–331.
- Liu, J., Y. Saito, X. Kong, H. Wang, C. Wen, Z. Yang, and R. Nakashima (2010), Delta development and channel incision during marine isotope stages 3 and 2 in the western South Yellow Sea, *Mar. Geol.*, *278*(1), 54–76.
- Liu, J. G., A. Li, and M. Chen (2010), Environmental evolution and impact of the Yellow River sediments on deposition in the Bohai Sea during the last deglaciation, *J. Asian Earth Sci.*, *38*(1), 26–33.
- Lupker, M., C. France-Lanord, V. Galy, J. Lavé, and H. Kudrass (2013), Increasing chemical weathering in the Himalayan system since the Last Glacial Maximum, *Earth Planet. Sci. Lett.*, *365*, 243–252.
- Makino Y. (1994), Wave ripple dynamics and the combined-flow modification of wave ripples in the intertidal zone of Ariake Bay (Kyushu, Japan), *Mar. Geol.*, *120*(1–2), 63–74.
- Meng, X., Y. Liu, X. Shi, and D. Du (2008), Nd and Sr isotopic compositions of sediments from the Yellow and Yangtze Rivers: Implications for partitioning tectonic terranes and crust weathering of the Central and Southeast China, *Front. Earth Sci. China*, *2*(4), 418–426.
- Meyer, I., G. R. Davies, and J.-B. W. Stuut (2011), Grain size control on Sr-Nd isotope provenance studies and impact on paleoclimate reconstructions: An example from deep-sea sediments offshore NW Africa, *Geochem. Geophys. Geosyst.*, *12*, Q03005, doi:10.1029/2010GC003355.
- Milliman, J. D., and K. L. Farnsworth (2011), *River Discharge to the Coastal Ocean: A Global Synthesis*, Cambridge Univ. Press, Cambridge, U. K.
- Milliman, J. D., C. P. Summerhayes, and H. T. Barretto (1975), Quaternary sedimentation on the Amazon continental margin: A model, *Geol. Soc. Am. Bull.*, *86*(5), 610–614.
- Milliman, J. D., Y. Qin, and Y. A. Park (1989), Sediments and sedimentary processes in the Yellow and East China Seas, in *Sedimentary Facies in the Active Plate Margin*, edited by A. Taira, and F. Masuda, pp. 233–249, Terra Sci., Tokyo.
- Moore, D. M., and R. C. Reynolds (1989), *X-ray Diffraction and the Identification and Analysis of Clay Minerals*, Oxford Univ. Press, Oxford.
- Nakai, S. I., A. N. Halliday, and D. K. Rea (1993), Provenance of dust in the Pacific Ocean, *Earth Planet. Sci. Lett.*, *119*(1), 143–157.
- Nie, J., T. Stevens, M. Rittner, D. Stockli, E. Garzanti, M. Limonta, A. Bird, S. Andò, P. Vermeesch, and J. Saylor (2015), Loess plateau storage of northeastern Tibetan plateau-derived Yellow River sediment, *Nat. Commun.*, *6*, 49–55.
- Oba, T., M. Kato, H. Kitazato, I. Koizumi, A. Omura, T. Sakai, and T. Takayama (1991), Paleoenvironmental changes in the Japan Sea during the last 85,000 years, *Paleoceanography*, *6*(4), 499–518.

- Ohtsubo, M., K. Egashira, and K. Kashima (1995), Depositional and post-depositional geochemistry, and its correlation with the geotechnical properties of marine clays in Ariake Bay, Japan, *Geotechnique*, *45*(3), 509–523.
- Okada, H., Y. Yasuda, M. Yagi, and K. Kai (2000), Geology and fluid chemistry of the Fushime geothermal field, Kyushu, Japan, *Geothermics*, *29*(2), 279–311.
- Park, Y., and B. Khim (1990), Clay minerals of the recent fine-grained sediments on the Korean continental shelves, *Cont. Shelf Res.*, *10*(12), 1179–1191.
- Qin, Y., and F. Li (1983), Study of influence of sediment loads discharged from the Huanghe River on sedimentation in the Bohai Sea and the Huanghai Sea, paper presented at Proceedings of the International Symposium on Sedimentation on the Continental Shelf with Special Reference to the East China Sea, China Ocean Press, Beijing.
- Rea, D., and T. Janecek (1981), Mass-accumulation rates of the non-authigenic inorganic crystalline (eolian) component of deep-sea sediments from the western Mid-Pacific Mountains, Deep Sea Drilling Project Site 463, *Initial Rep. Deep Sea Drill. Proj.*, *62*, 653–659.
- Reimer, P. J., et al. (2013), Intcal13 and Marine13 radiocarbon age calibration curves 0–50,000 years Cal BP, *Radiocarbon*, *55*(4), 1869–1887.
- Ren, M., and Y. Shi (1986), Sediment discharge of the Yellow River (China) and its effect on the sedimentation of the Bohai and the Yellow Sea, *Cont. Shelf Res.*, *6*(6), 785–810.
- Révilion, S., G. Jouet, G. Bayon, M. Rabineau, B. Dennielou, C. Hémond, and S. Berné (2011), The provenance of sediments in the Gulf of Lions, western Mediterranean Sea, *Geochem. Geophys. Geosyst.*, *12*, Q08006, doi:10.1029/2011GC003523.
- Saito, Y., H. Katayama, K. Ikehara, Y. Kato, E. Matsumoto, K. Oguri, M. Oda, and M. Yumoto (1998), Transgressive and high stand systems tracts and post-glacial transgression, the East China Sea, *Sediment. Geol.*, *122*(1), 217–232.
- Saito, Y., H. Wei, Y. Zhou, A. Nishimura, Y. Sato, and S. Yokota (2000), Delta progradation and chenier formation in the Huanghe (Yellow River) delta, China, *J. Asian Earth Sci.*, *18*(4), 489–497.
- Shi, X., Z. Yao, Q. Liu, J. C. Larrasoana, Y. Bai, Y. Liu, J. Liu, P. Cao, X. Li, and S. Qiao (2016), Sedimentary architecture of the Bohai Sea China over the last 1 Ma and implications for sea-level changes, *Earth Planet. Sci. Lett.*, *451*, 10–21.
- Sidle, R. C., and C. Masahiro (2004), Landslides and Debris Flows Strike Kyushu, Japan, *Eos Trans. AGU*, *85*(15), 145–151.
- Stuut, J. B. W., M. A. Prins, R. R. Schneider, G. J. Weltje, J. H. F. Jansen, and G. Postma (2002), A 300-kyr record of aridity and wind strength in southwestern Africa: Inferences from grain-size distributions of sediments on Walvis Ridge, SE Atlantic, *Mar. Geol.*, *180*(1–4), 221–233.
- Sun, J., and X. Zhu (2010), Temporal variations in Pb isotopes and trace element concentrations within Chinese eolian deposits during the past 8Ma: Implications for provenance change, *Earth Planet. Sci. Lett.*, *290*(3–4), 438–447.
- Sun, Y., D. W. Oppo, R. Xiang, W. Liu, and S. Gao (2005), Last deglaciation in the Okinawa Trough: Subtropical northwest Pacific link to Northern Hemisphere and tropical climate, *Paleoceanography*, *20*, PA4005, doi:10.1029/2004PA001061.
- Tada, R., T. Irino, and I. Koizumi (1999), Land-ocean linkages over orbital and millennial timescales recorded in Late Quaternary sediments of the Japan Sea, *Paleoceanography*, *14*(2), 236–247.
- Tada, R., et al. (2014), Asian Monsoon: Onset and evolution of millennial-scale variability of Asian monsoon and its possible relation with Himalaya and Tibetan Plateau uplift, *IODP Prelim. Rep.*, *346*, doi:10.2204/iodp.pr.346.2014.
- Ujiié, H., and Y. Ujiié (1999), Late Quaternary course changes of the Kuroshio Current in the Ryukyu Arc region, northwestern Pacific Ocean, *Mar. Micropaleontol.*, *37*(1), 23–40.
- Ujiié, H., Y. Tanaka, and T. Ono (1991), Late Quaternary paleoceanographic record from the middle Ryukyu Trench slope, northwest Pacific, *Mar. Micropaleontol.*, *18*(1), 115–128.
- Ujiié, Y., H. Ujiié, A. Taira, T. Nakamura, and K. Oguri (2003), Spatial and temporal variability of surface water in the Kuroshio source region, Pacific Ocean, over the past 21,000 years: Evidence from planktonic foraminifera, *Mar. Micropaleontol.*, *49*(4), 335–364.
- Walsh, J., and C. Nittrouer (2009), Understanding fine-grained river-sediment dispersal on continental margins, *Mar. Geol.*, *263*(1), 34–45.
- Wan, S., A. Li, P. D. Clift, and J.-B. W. Stuut (2007), Development of the East Asian monsoon: Mineralogical and sedimentologic records in the northern South China Sea since 20 Ma, *Palaeogeogr. Palaeoclimatol. Palaeoecol.*, *254*(3), 561–582.
- Wan, S., J. Tian, S. Steinke, A. Li, and T. Li (2010), Evolution and variability of the East Asian summer monsoon during the Pliocene: Evidence from clay mineral records of the South China Sea, *Palaeogeogr. Palaeoclimatol. Palaeoecol.*, *293*(1), 237–247.
- Wan, S., Z. Yu, P. D. Clift, H. Sun, A. Li, and T. Li (2012), History of Asian eolian input to the West Philippine Sea over the last one million years, *Palaeogeogr. Palaeoclimatol. Palaeoecol.*, *326*, 152–159.
- Wan, S., S. Toucanne, P. D. Clift, D. Zhao, G. Bayon, Z. Yu, G. Cai, X. Yin, S. Révilion, and D. Wang (2015), Human impact overwhelms long-term climate control of weathering and erosion in southwest China, *Geology*, *43*(5), 439–442.
- Wang, J., A. Li, K. Xu, X. Zheng, and J. Huang (2015), Clay mineral and grain size studies of sediment provenances and paleoenvironment evolution in the middle Okinawa Trough since 17 ka, *Mar. Geol.*, *366*, 49–61.
- Wang, P. (1999), Response of Western Pacific marginal seas to glacial cycles: Paleoenvironmental and sedimentological features, *Mar. Geol.*, *156*(1), 5–39.
- Wang, Y. J., H. Cheng, R. L. Edwards, Z. An, J. Wu, C.-C. Shen, and J. A. Dorale (2001), A high-resolution absolute-dated late Pleistocene monsoon record from Hulu Cave, China, *Science*, *294*(5550), 2345–2348.
- White, W. M., F. Albarède, and P. Télouk (2000), High-precision analysis of Pb isotope ratios by multi-collector ICP-MS, *Chem. Geol.*, *167*(3), 257–270.
- Xu, D. (1983), Mud sedimentation on the East China Sea shelf, paper presented at Proceedings of International Symposium on Sedimentation on the Continental Shelf with Special Reference to the East China Sea, China Ocean Press, Beijing.
- Xu, K., J. D. Milliman, A. Li, J. P. Liu, S.-J. Kao, and S. Wan (2009), Yangtze-and Taiwan-derived sediments on the inner shelf of East China Sea, *Cont. Shelf Res.*, *29*(18), 2240–2256.
- Xu, Z., T. Li, F. Chang, S. Wan, J. Choi, and D. Lim (2014), Clay-sized sediment provenance change in the northern Okinawa Trough since 22 kyr BP and its paleoenvironmental implication, *Palaeogeogr. Palaeoclimatol. Palaeoecol.*, *399*, 236–245.
- Yang, S., H. Jung, D. Lim, and C. Li (2003), A review on the provenance discrimination of sediments in the Yellow Sea, *Earth Sci. Rev.*, *63*(1), 93–120.
- Yang, S., C. Li, and J. Cai (2006), Geochemical compositions of core sediments in eastern China: Implication for Late Cenozoic palaeoenvironmental changes, *Palaeogeogr. Palaeoclimatol. Palaeoecol.*, *229*(4), 287–302.
- Yang, S., S. Jiang, H. Ling, X. Xia, M. Sun, and D. Wang (2007), Sr-Nd isotopic compositions of the Changjiang sediments: Implications for tracing sediment sources, *Sci. China Ser. D*, *50*(10), 1556–1565.
- Yang, Z. (1988), Clay mineral assemblages and chemical characters in Changjiang, Huanghe and Zhujiang sediments, and its relation with the climate environment in the source areas, *Oceanol. Limnol. Sin.*, *19*, 336–346.
- Yang, Z., Z. Guo, Z. Wang, J. Xu, and W. Gao (1992), Basic pattern of transport of sus-pended matter from the Yellow Sea and East China Sea to the eastern deep seas, *Acta Oceanol. Sin.*, *14*, 81–90.

- Yokoo, Y., T. Nakano, M. Nishikawa, and H. Quan (2004), Mineralogical variation of Sr-Nd isotopic and elemental compositions in loess and desert sand from the central Loess Plateau in China as a provenance tracer of wet and dry deposition in the northwestern Pacific, *Chem. Geol.*, 204(1–2), 45–62.
- Yokoyama, Y., T. Naruse, N. O. Ogawa, R. Tada, H. Kitazato, and N. Ohkouchi (2006), Dust influx reconstruction during the last 26,000 years inferred from a sedimentary leaf wax record from the Japan Sea, *Global Planet. Change*, 54(3), 239–250.
- Yoneda, M., H. Uno, Y. Shibata, R. Suzuki, Y. Kumamoto, K. Yoshida, T. Sasaki, A. Suzuki, and H. Kawahata (2007), Radiocarbon marine reservoir ages in the western Pacific estimated by pre-bomb molluscan shells, *Nucl. Instrum. Methods Phys. Res., Sect. B*, 259(1), 432–437.
- Yuan, D., J. Zhu, C. Li, and D. Hu (2008), Cross-shelf circulation in the Yellow and East China Seas indicated by MODIS satellite observations, *J. Mar. Syst.*, 70(1), 134–149.
- Zhang, J., W. W. Huang, M. G. Liu, and Q. Zhou (1990), Drainage basin weathering and major element transport of two large Chinese rivers (Huanghe and Changjiang), *J. Geophys. Res.*, 95(C8), 13,277–13,288.
- Zhang, Z., W. J. Ruan, and G. J. Jiang (1995), The relation of dynamic water flocculation settlement and bar deposition in Yangtze estuary, *Oceanol. Limnol. Sin.*, 26(6), 632–638.
- Zheng, X., A. Li, S. Wan, F. Jiang, S. J. Kao, and C. Johnson (2014), ITCZ and ENSO pacing on East Asian winter monsoon variation during the Holocene: Sedimentological evidence from the Okinawa Trough, *J. Geophys. Res. Oceans*, 119, 4410–4429, doi:10.1002/2013JC009603.
- Zheng, X., et al. (2016), Synchronicity of Kuroshio Current and climate system variability since the Last Glacial Maximum, *Earth Planet. Sci. Lett.*, 452, 247–257.
- Zhou, X., A. Li, S. Wan, and Q. Meng (2010), Clay minerals in surficial sediments of the East China Sea shelf: Distribution and provenance, *Oceanol. Limnol. Sin.*, 41, 667–675.